



Fisheries and Oceans
Canada

Pêches et Océans
Canada

Ecosystems and
Oceans Science

Sciences des écosystèmes
et des océans

Canadian Science Advisory Secretariat (CSAS)

Research Document 2025/057

National Capital Region

An Integrated Population Model for the Belcher Islands - Eastern Hudson Bay (BEL-EHB) Beluga Whale Stock

Joanie Van de Walle¹, M. Tim Tinker², and Caroline Sauvé¹

¹Maurice Lamontagne Institute
Fisheries and Oceans Canada
850, route de la Mer
Mont-Joli, Québec, G5H 3Z4

²Nhydra Ecological Consulting
St. Margaret's Bay, NS B3Z 2G6

Foreword

This series documents the scientific basis for the evaluation of aquatic resources and ecosystems in Canada. As such, it addresses the issues of the day in the time frames required and the documents it contains are not intended as definitive statements on the subjects addressed but rather as progress reports on ongoing investigations.

Published by:

Fisheries and Oceans Canada
Canadian Science Advisory Secretariat
200 Kent Street
Ottawa ON K1A 0E6

[http://www.dfo-mpo.gc.ca/csas-sccs/
DFO.CSAS-SCAS.MPO@dfo-mpo.gc.ca](http://www.dfo-mpo.gc.ca/csas-sccs/DFO.CSAS-SCAS.MPO@dfo-mpo.gc.ca)



© His Majesty the King in Right of Canada, as represented by the Minister of the Department of Fisheries and Oceans, 2025

This report is published under the [Open Government Licence - Canada](#)

ISSN 1919-5044

ISBN 978-0-660-78550-9 Cat. No. Fs70-5/2025-057E-PDF

Correct citation for this publication:

Van de Walle, J., Tinker, M.T., and Sauvé, C. 2025. An Integrated Population Model for the Belcher Islands - Eastern Hudson Bay (BEL-EHB) Beluga Whale Stock. DFO Can. Sci. Advis. Sec. Res. Doc. 2025/057. iv + 51 p.

Aussi disponible en français :

Van de Walle, J., Tinker, M.T., et Sauvé, C. 2025. Modèle de population intégré pour le stock de bélugas des îles Belcher et de l'est de la baie d'Hudson (BEL-EBH). Secr. can. des avis sci. du MPO. Doc. de rech. 2025/057. iv + 54 p.

TABLE OF CONTENTS

ABSTRACT	iv
INTRODUCTION	1
MATERIALS AND METHODS	2
BELUGA LIFE CYCLE	2
DATA SOURCES	3
Abundance from aerial surveys.....	3
Pregnancy rates	3
Harvest numbers	3
Genetic composition of the harvest.....	4
Harvest sex and age structure	4
Proportion of lactating females in the harvest.....	5
MODEL CONSTRUCTION.....	5
Process model	5
Survival as competing hazards	7
Pregnancy rates	9
DATA MODEL	10
PRIORS	12
MODEL ANALYSIS	13
Model Fitting and validation	13
Model analysis and scenarios	13
RESULTS	14
POPULATION DYNAMICS UNDER THE IPM.....	14
COMPARISON BETWEEN IPM AND SPM	15
DISCUSSION.....	16
REFERENCES CITED.....	20
TABLES	25
FIGURES	30
APPENDIX.....	42
MULTISTATE MODEL CONSTRUCTION	42
TRANSITIONS OF LIVE INDIVIDUALS.....	42
REPRODUCTION PROCESSES.....	43

ABSTRACT

The Belcher Islands Eastern Hudson Bay (BEL-EHB) beluga stock is one of eight stocks found in Canada. It is one of the least abundant, with Eastern Hudson Bay beluga being currently designated as Threatened by COSEWIC. The BEL-EHB stock is harvested for subsistence by Nunavik communities and the Nunavut community of Sanikiluaq. Population models are used to estimate the population abundance and trend of the BEL-EHB stock, and to provide scientific advice on harvest levels compatible with identified management objectives. The BEL-EHB stock was last assessed using a stochastic Bayesian surplus-production model (SPM) incorporating information on harvest numbers, genetic-based composition of the harvest and aerial survey estimates. Several additional sources of information have now become available and can be used to produce a more comprehensive assessment of the stock. Here, we developed a new Integrated Population Model (IPM) for BEL-EHB beluga that integrates female reproductive status, as well as harvest sex and age composition as additional sources of information into the model structure. In addition, annual stochasticity was incorporated in the IPM as a component of mortality in addition to harvesting. We present the structure of the newly developed IPM and then compare the modeled population trends and abundance estimates to those from the SPM used in previous assessments. The IPM and SPM predicted similar overall population abundances and trends. However, uncertainties in model-based predictions were reduced with the IPM, and the most recent estimates of abundance diverged between modeling approaches. The IPM predicted that the BEL-EHB stock abundance was 3,600 in 2023, with a rate of decline between 2014-2023 corresponding to 2.24%. The 2023 estimate of BEL-EHB abundance using the SPM was 2,600 and the rate of decline between 2014-2023 was 3.82%. Both models yielded similar predictions of BEL-EHB beluga landings and carrying capacity. The IPM provided new information about the BEL-EHB stock that could not be obtained with the SPM. For instance, the IPM yielded insights into age-specific survival and pregnancy rates, as well as temporal trends in those demographic rates. Further, the IPM estimated that mortality resulting from harvest (including struck and lost) accounts for 19% to 43% of total annual mortality, with an increasing trend in recent years.

INTRODUCTION

The beluga (*Delphinapterus leucas*) is widely distributed across Arctic and subarctic waters, with a substantial proportion of its global range distributed in Canadian waters (NAMMCO 2018; Hobbs et al. 2019). The delineation of designatable units (DUs), populations and management stocks is based on the fragmented distribution of summering aggregations (Sergeant 1973; Finley et al. 1982; Reeves and Mitchell 1987; Richard 2010). These divisions are supported by evidence that beluga display strong intra- and inter-annual site fidelity to summering grounds, based on behavioural observations (Caron and Smith 1990), telemetry (Bailleul et al. 2012a), stable isotopes and contaminant analyses (Rioux et al. 2012), and genetic studies (Brennin et al. 1997; Brown Gladden et al. 1997, 1999; de March et al. 2002, 2004; de March and Postma 2003; Postma et al. 2012; Turgeon et al. 2012; Colbeck et al. 2013; Parent et al. 2023).

The Committee on the Status of Endangered Wildlife in Canada (COSEWIC) has identified eight beluga DUs in Canada, including four occurring in the waters adjacent to Nunavik (northern Quebec) at different periods throughout the year: Western Hudson Bay (WHB), Eastern Hudson Bay (EHB), James Bay (JB) and Ungava Bay (UB) (COSEWIC 2016). The EHB DU is one of the least abundant and is currently designated as Threatened (COSEWIC 2020). Since the last COSEWIC beluga DU review in 2020, a genetic re-analysis by the Department of Fisheries and Oceans Canada (DFO) has identified two distinct genetic populations of beluga within the EHB DU's geographic summer distribution: an EHB and a Belcher Islands (BEL) population (Parent et al. 2023). Because the BEL and EHB genetic populations show strong overlap in summer distribution and cannot be distinguished during aerial surveys to produce separate abundance estimates of beluga in the area, they are managed together as a BEL-EHB stock (Hammill et al. 2023b; Sauvé et al. 2024).

Beluga are culturally significant to Nunavik Inuit, serving as a nutritive food source and being integral to traditional practices and social cohesion (Tyrrell 2007, 2008; Lemire et al. 2015; Breton-Honeyman et al. 2016). Since the signing of the Nunavik Inuit Land Claim Agreement (NILCA) in 2006, the beluga harvest in northern Quebec waters is co-managed by the Wildlife Management Boards (i.e., the Nunavik Marine Region Wildlife Board (NMRWB) in the NILCA region and jointly with the Eeyou Marine Region Wildlife Board in the areas where the land claims overlap) and DFO, balancing harvesting rights with conservation objectives.

BEL-EHB beluga summer in the estuaries and offshore waters of the eastern Hudson Bay Arc (i.e., the curved segment of southeastern Hudson Bay, extending from Hopewell Islands to the junction with James Bay and can be seen up to 60 km west of the Belcher Islands (Figure 1; Bailleul et al. 2012b). Historically, the largest aggregations were observed in July and August in Lake Tasiujaq (formerly known as Richmond Gulf), Little and Great Whale rivers, and the Nastapoka River (Smith and Hammill 1986; Caron and Smith 1990). Commercial overharvesting decimated the beluga summering in Great Whale River in the 19th century, (Reeves and Mitchell 1987). While occasional sightings are still reported in the Nastapoka River estuary, no beluga have been observed there during aerial surveys since 2004 (Gosselin et al. 2017; COSEWIC 2020; St-Pierre et al. 2024). Currently, the Little Whale River estuary appears to be the principal site for beluga aggregations in the eastern Hudson Bay Arc. In fall, beluga from eastern Hudson Bay migrate along the Nunavik coast, into Hudson Strait sometimes entering Ungava Bay before overwintering in Hudson Strait and along the Labrador coast where they overlap with beluga from other stocks (Lewis et al. 2009; Bailleul et al. 2012a; Parent et al. 2023).

BEL-EHB beluga are harvested by hunters in Nunavik and Nunavut (Sanikiluaq) while in their summering areas, and along their migration route (Figure 2). Given the presence of beluga from other DUs around Nunavik, the proportion of BEL-EHB beluga in the total beluga harvest differs

across the different management areas and seasons. Since the 1980s, harvesters across Nunavik and Nunavut have contributed skin samples from their catches, which have been used to provide insights into the genetic structure of beluga in the Canadian Arctic. Samples from Nunavik and Sanikiluaq have been used to estimate the relative proportion of the different beluga stocks found in the harvest in the different management areas (Brown Gladden et al. 1997; de March et al. 2002, 2004; de March and Postma 2003; Turgeon et al. 2009, 2012; Postma et al. 2012; Postma 2017; Parent et al. 2023).

The status of the BEL-EHB stock was last assessed in 2021 using a stochastic Bayesian Surplus-Production Model (SPM) incorporating information on catches, genetic-based stock composition and aerial survey estimates (Hammill et al. 2023b). However, the availability of several new data sources now allows for a more comprehensive assessment. Specifically, in addition to a skin sample and information on sex and sample location, hunters provide a tooth (which can be used for age estimation) and a blubber sample. Recent advances in quantification of blubber progesterone levels have been used to estimate pregnancy status in beluga (Goertz et al. 2019; Renaud et al. 2023).

In an effort to improve our understanding of the dynamics of the EHB-BEL beluga stock, we developed an Integrated Population Model (IPM) for BEL-EHB beluga that integrates data on harvest composition (i.e., age, sex and female reproductive status) as additional sources of information into the model structure. This new model follows recent developments in population modelling for grey seals (Hammill et al. 2023a), harp seals (Tinker et al. 2023) and St. Lawrence Estuary beluga (Tinker et al. 2024). In addition to optimizing the use of available information from sampled beluga and increasing the consistency in approaches used to model marine mammal stocks nationally, this new model provides a framework that can integrate environmental stochasticity as a factor influencing population dynamics, which addresses a request made by co-management partners. The objective of this paper is to present the structure of the newly developed IPM for BEL-EHB beluga and then compare the modeled population trends and abundance estimates to those from the SPM used in previous assessments (e.g., Hammill et al. 2023b).

MATERIALS AND METHODS

The methods section is divided into four subsections: we present the beluga life cycle, the different sources of data that are used to inform the population model, the model structure and, finally, the methods used for model validation and fit, including comparisons of model estimates with those from the BEL-EHB beluga SPM.

BELUGA LIFE CYCLE

Beluga females reach sexual maturity between 8-14 years-old (Sergeant 1973; Doidge 1990; Ferguson et al. 2020). The timing of mating and calving varies among populations, but mating generally occurs in late winter and spring and calving during summer. Beluga from eastern Hudson Bay are thought to mate in early May. Calving occurs the following year from late May through August, with a peak in June (Doidge 1990). Females give birth to a single calf after a gestation duration of approximately 12.8-15 months (Doidge 1990; Matthews and Ferguson 2015). Lactation typically lasts about two years (Doidge 1990; Matthews and Ferguson 2015), and thus the inter-birth interval (assuming calf survival) is approximately three years (Doidge 1990; Matthews and Ferguson 2015). However, if the calf dies, the female can become pregnant again, reducing the reproductive cycle to two years (Mosnier et al. 2015). Beluga are born with a dark grey or brown coloration and gradually transition to a white coloration towards 10-20 years of age (COSEWIC 2020). Longevity is between 45-89 years (McAlpine et al. 1999;

Lesage et al. 2014; Hobbs et al. 2015; Ferguson et al. 2020). The beluga is one of the rare species where females show signs of post-reproductive lifespan (Ellis et al. 2018). However, there is variability in age of reproductive senescence, which can be as early as 35-50 years of age, although pregnant females aged 60-70 years have been reported (Burns and Seaman 1986; Ellis et al. 2018; Ferguson et al. 2020).

DATA SOURCES

The IPM uses six sources of data:

1. Abundance from aerial surveys,
2. Pregnancy rates,
3. Harvest numbers,
4. Genetic composition of the harvest,
5. Harvest sex and age structure, and
6. Proportion of adult females lactating in the harvest.

Abundance from aerial surveys

Abundance of beluga in eastern Hudson Bay is estimated from systematic, visual line-transect aerial surveys. These surveys are flown from the eastern Hudson Bay coast to 60 km west of the Belcher Islands, and therefore are considered to inventory both the BEL and EHB populations (i.e., the BEL-EHB stock) over the entire extent of their summer distribution. A total of 8 summer surveys have been conducted since 1985 (1985, 1993, 2001, 2004, 2008, 2011, 2015 and 2021), as summarized in (St-Pierre et al. 2024). See Table 1 for survey estimates and associated uncertainties.

Pregnancy rates

Annual pregnancy rates were estimated by quantifying progesterone levels in blubber samples collected from 118 mature (i.e., older than eight years of age, with age being determined from dental analyses; Doidge 1990; Heide-Jørgensen and Teilmann 1994) female beluga harvested along the Nunavik coast from 2010-2022. Briefly, pregnant females have higher blubber progesterone levels, compared to resting and lactating females (Goertz et al. 2019). Progesterone levels can remain high for some time post-parturition (Renaud et al. 2023). Also, because gestation extends over a year in beluga females in early- and late-term pregnancy stages co-occur during summer. To avoid overestimating annual pregnancy rates and misclassifying post-parturient females as pregnant, we only considered samples collected between the months of October through April. Blubber progesterone extraction and quantification followed the methods described in Renaud et al. (2023). A progesterone level threshold of 100 ng/g of tissue was used to determine presumed pregnancy, which has previously been associated with a misclassification rate of 6% (Renaud et al. 2023). Presumed pregnant and non-pregnant females were summed separately for each year. Sample sizes for annual reproductive rates ranged between 2 and 30 (Table 2).

Harvest numbers

Harvest information is collected yearly from each community via a network of local wardens in Nunavik (1974-2023) and via the Sanikiluaq Hunters and Trappers Association (1977-2023), and then combined to yield harvest numbers for management areas where BEL-EHB are harvested: Sanikiluaq (SAN), Eastern Hudson Bay including the Kuujjuarapik pilot area and the

Northeastern Hudson Bay voluntary closure zone (referred to as the ARC), Northeastern Hudson Bay except the voluntary closure zone (NEHB), Hudson Strait (HS), and Ungava Bay (UB) (Figure 2; Table 3). For SAN, harvest outside of summer was divided into spring (April 1st through June 30th), fall (September 1st through November 30th) and winter (December 1st through March 31st) periods. Prior to 2023, total annual SAN harvest numbers were broken down by season following the relative proportion of all genetic samples that were collected in each season. In 2023, harvest numbers for SAN were available on a monthly basis, allowing for the compilation of season-specific numbers directly. For HS, NEHB and UB, harvest was assigned to spring (February 1st through August 31st) and fall (September 1st through January 31st) migration periods. Only total annual harvest was available for HS up to 2008, while season-specific (spring vs fall) harvest numbers were available from 2009 onward. We back-calculated the proportion of the harvest taken during the spring vs the fall seasons for 1974-2008 using the overall season-specific proportions from the 2009-2023 period.

Genetic composition of the harvest

SAN and ARC areas combined correspond to the BEL-EHB summering grounds, therefore all beluga harvested in these areas are defined as BEL-EHB beluga. In contrast, NEHB, HS and UB areas are located along the migratory path and wintering grounds of BEL-EHB beluga, which are also shared with other beluga stocks. Harvests from these areas therefore represent a mix of beluga belonging to various stocks. Tissue samples from 1982-2021 were haplotyped for the mitochondrial DNA control region (Parent et al. 2023). Samples collected during summer (July and August) in SAN and ARC were used as the reference group for BEL-EHB beluga haplotype composition, which was introduced as input for a Genetic Mixture Analysis (GMA) to assess the proportion of BEL-EHB beluga in other seasons and management areas (Parent et al., 2023; Table 4).

Sample size was insufficient ($n < 10$) to estimate the proportion of BEL-EHB from harvests carried out in NEHB during the spring and in UB during the fall. For those harvests, we calculated a proportional BEL-EHB contribution based on the fall and spring estimates from HS, respectively. Further, harvest numbers in SAN were available only on an annual basis up to 2022, but the proportion of BEL-EHB is assessed for each season. Harvest numbers were thus broken down by season according to the relative proportion of the genetic samples that came from each season. We calculated the proportion of the harvest that came from the spring vs the fall using the 2009-2023 period to back-calculate the season-specific harvest numbers for the period 1974-2008. Finally, using the high number of samples collected in Hudson Strait over the time series, Parent et al. (2023) found that the proportion of BEL-EHB harvested in HS during fall declines after the second week in November. Therefore, we separated the fall season into “early fall” (Sept. 1 - Nov. 20) and “late fall” (Nov. 21 - Jan. 31) seasons for years 2018 onward, when weekly harvest reports were available, to account for this (Table 4). We used both the mean estimates of proportional representation of BEL-EHB as well as associated uncertainties (estimator variance) for calculating harvest mortality of BEL-EHB beluga in our model, as described below.

Harvest sex and age structure

For a proportion of beluga harvested between 1980-2023 (66%; 2,203 out of 3,327), information on sex and age were available. Age was determined based on dental analysis as in Lesage et al. (2014) and was used to determine the age structure among the sample of harvested beluga (Figure 3).

Proportion of lactating females in the harvest

The management plan for Nunavik beluga and Marine Mammal Regulations state that no person shall hunt a beluga calf (dark color), or an adult beluga that is accompanied by a calf. Accordingly, a bias towards non-lactating females is expected in the harvest and the IPM accounts for an avoidance of lactating females. To inform the model on this avoidance factor, we used data collected on a subset of white and light grey beluga females harvested in Quaqtaq in 2023 ($n = 21$) and 2024 ($n = 17$) and necropsied by DFO personnel. For each harvested female, lactation status was assessed by visual inspection of the mammary glands and detection of milk in the glands. In 2023 and 2024, 3 (18%) and 2 (10%) of necropsied females were lactating, respectively.

MODEL CONSTRUCTION

We used a Bayesian IPM that integrates multiple sources of data to estimate population abundance of the BEL-EHB stock. The IPM is comprised of three parts:

1. Process model,
2. Data model and
3. Model fitting.

The process model is a series of equations that describe demographic transitions and which, when solved, estimates dynamics in population abundance based on the values of the input parameters. The data model describes how the empirical datasets are linked to the predicted dynamics of the process model. The model fitting part describes how input parameters are estimated. Note that vectors and matrices are presented in bold characters, and \odot represents the element-by-element vector multiplication.

Process model

We used a multi-state population model, as formulated by Caswell et al. (2018) and Roth and Caswell (2016). In this formulation, individuals are classified within two or more dimensions simultaneously. For beluga, we characterized individuals along two distinct dimensions: age class (i) and a combination of sex and reproductive state (hereafter referred to as “state”; j);

Dimension 1, $i, \in \{1, \dots, w\}$

Dimension 2, $j, \in \{1, \dots, b\}$

We considered 61 age classes ($w = 61$). Each age class was of length 1 year, except the last one which was left open-ended and included individuals of age ≥ 60 years old, age at which pregnancy is rare (Suydam 2009).

We considered four states ($b = 4$):

1. males (M),
2. non-reproducing females (A),
3. pregnant females (P) and
4. females with a calf (W).

The model includes males in its formulation as a single and distinct state to account for sex-specific differences in survival. The model tracks male abundance over time, but males are not separated according to their reproductive state. In contrast, females are separated into three reproductive states, following Mosnier et al. (2015), to account for potential differential

constraints acting on females at different reproductive stages of their life cycle. Non-reproducing females (A) include immature females and adult females that are either not pregnant or caring for a calf. Females can only reach the states P and W at the minimal ages of 8 and 9, respectively. Transitions between states occur during an annual time step, which is between the periods of census at times t and $t + 1$. Census time is set at the time of aerial surveys, i.e., in late summer, hence the model considers a post-breeding census. Therefore, at the time of census, calves of the year are born and only early pregnancies are present. Transitions between states and fertilities (i.e., the production of new individuals) are presented in Figure 4.

The vector $\tilde{\mathbf{n}}$ contains the number of individuals within each combination of age class i and state j . The vector $\tilde{\mathbf{n}}$ is of length k , with $k = w \times b$. The multistate matrix $\tilde{\mathbf{A}}$ projects the population vector $\tilde{\mathbf{n}}$ forward in time, from time t to time $t + 1$ and has the same structure,

$$\tilde{\mathbf{n}}(t + 1) = \tilde{\mathbf{A}}(t)\tilde{\mathbf{n}}(t) \quad (1)$$

The construction of the multistate projection matrix relies on the separation of processes (i.e., transitions of live individuals and production of offspring through reproduction) occurring in the different dimensions (i.e., age and state). Annual transitions are conditional on age- and state-specific survival rates and for females on age-specific probabilities of becoming pregnant. Details on the construction of the multistate projection matrix are presented in Appendix 1. Briefly, we considered four sets of matrices (two processes occurring along two dimensions):

1. ageing (**U** matrices),
2. state transitions (**B** matrices),
3. reproduction (**R** matrices) and
4. offspring sex attribution (**F** matrices).

First, the \mathbf{U}_j matrices are built for each state j at each time step t . They contain age- and state-specific survival probabilities (S) on the sub-diagonal.

$$\mathbf{U}_j(t) = \begin{pmatrix} 0 & \dots & 0 & 0 & 0 \\ S_{1,j}(t) \times SW & \dots & 0 & 0 & 0 \\ \vdots & \ddots & \vdots & \vdots & \vdots \\ 0 & \dots & S_{w-2,j}(t) & 0 & 0 \\ 0 & \dots & 0 & S_{w-1,j}(t) & S_{w,j}(t) \end{pmatrix} \quad (2)$$

Note that beluga reach sexual maturity at age 8 years old. Therefore, considering that age class 1 consists of 0 year-olds, females can only reach state P (pregnant female) once in age class 9 (corresponding to age 8 years-old). The state W (female with a calf) can then only be attained upon reaching age class 10. Therefore, the parameter S was set to 0 for P of age classes 1 through 8 and for W of age classes 1 through 9.

Beluga are weaned either after 1 or 2 years of lactation (Matthews and Ferguson 2015). While calves mostly rely on lactation during their first year, most beluga consume a mixture of milk and solid food during their second year of life and one third of calves are completely weaned after their first year. This suggests that beluga may be fully dependent on maternal provisioning during their first year of life, but may become independent in their second year. We thus assumed that the survival of calves (age 0 individuals, corresponding to age class 1) to the next year was conditional on the survival of their mother (SW). SW was estimated as the weighted average survival of W females, with weight corresponding to the estimated proportion of W females in each age class at the current year.

Second, the \mathbf{B}_i matrices are built for each age class i at each time step t . They contain the age-specific probabilities of transitioning between the four states, j (M, A, P and W), acknowledging this probability is zero for males. For females, those probabilities are conditional on pregnancy rates (Pr) and neonatal mortality (S_n), as pregnant females at time t may become pregnant again at time $t + 1$ if they lose their calf in the time interval.

$$\mathbf{B}_i(t) = \begin{pmatrix} 1 & 0 & 0 & 0 \\ 0 & 1 - Pr_i(t) & 1 - S_n(t) & 1 \\ 0 & Pr_i(t) & 0 & 0 \\ 0 & 0 & S_n(t) & 0 \end{pmatrix} \quad (3)$$

Note that for i in $1 - 8$, Pr_i was set to zero.

Third, the \mathbf{R}_j matrices are built for each state j at each time step t . They contain the state-specific probabilities of producing individuals of the first age-class, i.e., calves. Only pregnant females ($j = P$) can produce calves, so \mathbf{R}_j for $j \in (M, A, W)$ are zero matrices. In the \mathbf{R} matrix for pregnant females, females at time t can give birth to a calf and reach the state W at time $t + 1$ conditional on their survival (S) and that of their neonate (S_n) until population census.

$$\mathbf{R}_j(t) = \begin{pmatrix} S_{1,3}(t) \times S_n(t) & S_{2,3}(t) \times S_n(t) & \cdots & S_{w,3}(t) \times S_n(t) \\ 0 & 0 & \cdots & 0 \\ \vdots & \vdots & \ddots & \vdots \\ 0 & 0 & \cdots & 0 \end{pmatrix} \quad (4)$$

Fourth, the \mathbf{F}_i matrices assign newly produced offspring to either the M or A states:

$$\mathbf{F}_i = \begin{pmatrix} 0 & 0 & \tau & 0 \\ 0 & 0 & 1 - \tau & 0 \\ 0 & 0 & 0 & 0 \\ 0 & 0 & 0 & 0 \end{pmatrix} \quad (5)$$

with τ being the probability that newly produced offspring are males. We assumed an equal sex ratio at birth, so τ was fixed at 0.5.

The \mathbf{U} , \mathbf{B} , \mathbf{R} , and \mathbf{F} matrices are assembled into block-matrices and then multiplied together to generate an age \times state multistate projection matrix (Roth and Caswell 2016; Caswell et al. 2018). See Appendix 1 for more details on the construction of the multistate projection matrix and Figure A1 for a visual representation of the matrix.

Survival as competing hazards

Survival was computed in terms of instantaneous hazards, following Tinker et al. (2024). In this framework, mortality is the result of multiple competing hazards (Λ). Each hazard represents one distinct additive source of instantaneous mortality. We considered two sources of additive mortality: 1) natural or environmental mortality (hereafter referred to as baseline hazards; Λ_B), and 2) hunting mortality (hereafter referred to as hunting hazards; Λ_H). Hazards are given in their log form as this allowed the inclusion of predictor variables as simple additive linear functions. Survival rates are then given by the exponential of the negative sum of all instantaneous hazards. Each source of hazard is described in more detail below.

Baseline hazards

Age-specific baseline hazards (Λ_B) are calculated for each state (j) at each time step (t) as follows:

$$\log(\Lambda_{B,j}(t)) = \zeta + \gamma_0 + \gamma_1 \cdot \Delta_j + \gamma_2 \cdot \Omega_j + \gamma_3 \cdot \Gamma_j + \Delta_j \cdot \left[\phi \cdot \left(\frac{N(t)}{1000} \right) + \sigma_e \cdot \epsilon_e(t) \right] \quad (6)$$

The parameter ζ is a minimum log hazard rate set to an arbitrarily low value (here $\zeta = -10$, which corresponds to an annual survival rate > 0.9999). The inclusion of this parameter allows all remaining terms to be interpreted as log hazard ratios with respect to this minimum. The parameter γ_0 corresponds to the baseline adult mortality. Differential hazards in early and late life are captured by the terms $\gamma_1 \cdot \Delta_j$ and $\gamma_2 \cdot \Omega_j$, respectively. The parameters γ_1 and γ_2 correspond to the effects of early and late hazards, respectively, while Δ_j and Ω_j are age-modifying vectors of length w . Age-modifying vectors are the same across all values of j and are further described below in equations 7-9.

We accounted for potential sex-specific differences in adult survival rates (Tinker et al. 2024) by including the parameter γ_3 , which corresponds to the log hazard ratio for adult males relative to adult females. The parameter γ_3 only applies to adult males, which is ensured by the vector Γ_j which for $j \in \{A, P, W\}$ has zeros in all entries and for $j = M$ has ones in entries corresponding to adults and zeros elsewhere.

We estimated the magnitude of density-dependent effects on mortality via parameter ϕ , which was multiplied by population size in thousands, $N(t)/1000$. We accounted for environmental stochasticity by including random effect $\sigma_e \cdot \epsilon_e(t)$, where σ_e represents the magnitude of environmental stochasticity and $\epsilon_e(t)$ is a normal random variate with unit variance. Density-dependent effects and environmental stochasticity are more likely to impact the survival of younger age classes (Eberhardt 2002; Lair et al. 2015). Therefore, we scaled these effects to age by multiplication with age-modifying vector Δ_j , which increases hazards for younger individuals:

$$\Delta_j = \frac{\widehat{\Delta}_j - \min(\widehat{\Delta}_j)}{\max(\widehat{\Delta}_j) - \min(\widehat{\Delta}_j)} \quad (7)$$

$$\text{and } \widehat{\Delta}_j = e^{\delta \cdot \log\left(\frac{1}{v_j}\right)} \quad (8)$$

The age-modifying vector Ω_j , which increases hazards for older individuals, was calculated as:

$$\Omega_j = \frac{v_j^{\omega+1}}{\max(v_j)^{\omega+1}} \quad (9)$$

In Equations 8 and 9, the vector v_j is the vector of age classes of length w , while the parameters δ and ω determine the degree of non-linearity in the functional forms of Δ_j and Ω_j .

Harvest hazards

Harvest mortality was included as a separate hazard, Λ_H , for each state j , and each year t , as follows:

$$\log(\Lambda_{H,j}(t)) = \zeta + \gamma_H + \sigma_H \cdot \epsilon_H(t) + \log(\Theta_j) \quad (10)$$

In equation 10, ζ corresponds to the minimum log hazard, as defined in equation 6. The parameter γ_H is the mean log hazard ratio associated with harvest mortality. Parameter σ_H is the magnitude of variation in harvest hazards and $\epsilon_H(t)$ is a random effect (normally distributed with unit variance) accounting for annual fluctuations in harvest hazards.

The age distribution of harvested and sampled individuals presents a noticeable under representation of younger age classes (Figure 3). This may be attributed to hunters actively avoiding calves and juveniles, as outlined in the Marine Mammal Regulations (SOR/93-56) and in the Nunavik beluga management plan, and because larger animals provide more food (Regional Anguvigaq and Anguvigarait, *pers. comm.*). We accounted for this age bias in harvesting by multiplying the harvest hazard function with the age-modifying vector Θ , which increases the strength of the harvest mortality hazard as individuals age. The parameter Θ is of length w , ranges from 0 to 1 and was calculated as follows:

$$\theta_j = \frac{1}{1 + e^{-(-10 + \psi_1 + \psi_2 \cdot v_j)}} \quad (11)$$

where ψ_1 and ψ_2 are parameters to be estimated by the model and characterize the functional relationship between age and harvest hazards.

Survival rates

For males, non-reproducing females and pregnant females (i.e., $j \in \{M, A, P\}$), hazards were back-transformed to an age varying vector of survival rates at each time step t as follows:

$$S_j(t) = e^{-(\Lambda_{B,j}(t) + \Lambda_{H,j}(t))} \quad (12.1)$$

We note that the survival rate for first year calves was further modified to account for the mothers survival rate, as shown in equation 2. To account for the potential avoidance of females with calves by hunters, harvest hazards were multiplied by a bias factor, ξ , which represents the proportional reduction in harvest-related hazard for state W relative to other states, as follows:

$$S_W(t) = e^{-(\Lambda_{B,W}(t) + \Lambda_{H,W}(t) \cdot \xi)} \quad (12.2)$$

Pregnant females at time t will give birth over the summer, while censuses occur at the end of the summer. If a female loses her calf in the time interval between birth and census, the female could be in state A at census time. Therefore, we also calculated neonate survival S_n as a fraction of survival rate of yearling males at every year t :

$$S_n(t) = S_{1,1}(t)^{0.1} \quad (13)$$

Pregnancy rates

Non-reproducing females ($j = A$) can become pregnant between year t and year $t + 1$, conditional on their survival and pregnancy probability, Pr . We used the same approach as for hazards to model the probability of becoming pregnant, only here "hazards" (Λ_{Pr}) correspond to the instantaneous probability of *not* becoming pregnant. Λ_{Pr} was calculated as follows:

$$\log(\Lambda_{Pr}(t)) = \eta + \rho \cdot \phi \cdot \left(\frac{N(t)}{1000} + \sigma_e \cdot \epsilon_e(t) \right) \quad (14)$$

and

$$Pr(t) = e^{-\Lambda_{Pr}(t)} \cdot \Upsilon \quad (15)$$

where Υ is an age-modifying vector of length w accounting for age variation factors in pregnancy rates such as an absence of reproductive activity before 8 years-old ($\Upsilon_{1-7} = 0$) and a decline in pregnancy rates with age (i.e., senescence). Equation 14 includes baseline pregnancy hazards (h) and the effects of density dependence and environmental stochasticity, assumed to be proportional to the density-dependent and stochastic effects described for juvenile survival (equation 6) but scaled by parameter r .

DATA MODEL

The process model was fitted to the different sources of data, i.e., abundance estimates, harvest levels along with their genetic composition, demographic composition (age and sex structure, as well as proportion of adult females lactating). We defined probabilistic relationships between each data set and the corresponding predictions generated by the process model.

The uncertainty distributions associated with survey estimates followed a lognormal distribution, thus we related the observed point estimates from aerial surveys ($ObsS(t)$) to the model-estimated abundance values ($N(t)$) using a lognormal distribution:

$$ObsS(t) \sim \text{lognormal} \left(\mu = \log \left(\frac{N(t)^2}{\sqrt{N(t)^2 + SE(t)^2}} \right), \sigma = \left(\sqrt{\log \left(1 + \frac{SE(t)^2}{N(t)^2} \right)} \right) \right) \quad (16)$$

where $SE(t)$ represents the standard error estimate computed separately for each aerial survey (St-Pierre et al. 2024).

The observed proportion of females pregnant in the harvest sample at time t ($NPr(t)$) was related to the expected proportion of harvested females that are pregnant ($PPr(t)$) using a beta-binomial distribution:

$$NPr(t) \sim \text{betabinomial}(NAF(t), \alpha, \beta), \quad (17)$$

where

$$\alpha = v_{Pr} \cdot Prop_{BE}(t)^2 \cdot PPr(t) \quad (18)$$

and

$$\beta = v_{Pr} \cdot Prop_{BE}(t)^2 \cdot (1 - PPr(t)) \quad (19)$$

where $NAF(t)$ is the observed number of adult females sampled, v_{Pr} is the precision of pregnancy rates proportions, and $Prop_{BE}(t)$ is the estimated proportion of the sample from the BEL-EHB stock. The realized precision of equation 17 is thus assumed to depend on the proportion of the sample comprised of BEL-EHB animals: the higher this fraction, the more we expect the observed pregnancy rates to reflect the model-estimated pregnancy rates for the BEL-EHB stock. $Prop_{BE}(t)$ is calculated as follows:

$$Prop_{BE}(t) = \sum (P_H(t) \odot P_{BE}(t)) \quad (20)$$

where $P_H(t)$ is the yearly proportion of total hunt by area/season and $P_{BE}(t)$ is the genetically-determined proportion of individuals attributed to the BEL-EHB stock by area/season for each year. To account for uncertainty in genetic-based composition estimates, $P_{BE}(t)$ is itself treated as an estimated parameter drawn from a beta distribution with mean and variance corresponding to the mean values and estimator variances reported by Parent et al. (2023).

The total reported number of animals harvested throughout Nunavik and in Sanikiluaq at each year t , $HarvO(t)$, is assumed to follow a Poisson distribution with an expected mean corresponding to the model-based estimate of total number of beluga harvested each year ($HarvE(t)$):

$$HarvO(t) \sim \text{Poisson}(HarvE(t)) \quad (21)$$

with

$$HarvE(t) = \sum \left(\tilde{\mathbf{d}}(t) \odot \left(\frac{\mathbf{\Lambda}_H(t)}{\mathbf{\Lambda}_H(t) + \mathbf{\Lambda}_B(t)} \right) \right) \cdot \frac{Q}{Prop_{BE}(t)} \quad (22)$$

and

$$\tilde{\mathbf{d}}(t) = \tilde{\mathbf{M}}(t) \cdot \tilde{\mathbf{n}}(t-1) \quad (23)$$

Specifically, we multiplied the population vector at year $t-1$, $\tilde{\mathbf{n}}(t-1)$, with a mortality matrix, $\tilde{\mathbf{M}}(t)$, of the same dimension as the $\tilde{\mathbf{A}}$ matrix ($w \times b$ by $w \times b$). The $\tilde{\mathbf{M}}(t)$ matrix only contains mortality probabilities at year t from all hazards combined on the diagonal, so that its multiplication with the vector $\tilde{\mathbf{n}}(t-1)$ gives the vector of beluga that died at year t , $\tilde{\mathbf{d}}(t)$. To obtain the harvest-related number of deaths ($HarvE(t)$), we multiplied this vector by the proportion of hazards associated with harvest over all sources of hazard. Here, the vectors $\mathbf{\Lambda}_B$ and $\mathbf{\Lambda}_H$ contain the baseline and harvest hazards arranged for states M, A, P and W, so that their respective lengths are $w \times b = 240$. This gives the total mortality that is attributed to harvest. This is then multiplied by Q , which is the inverse of the proportion of beluga struck and lost (SnL) to provide the number of BEL-EHB beluga that were landed and reported. SnL is the proportion of animals killed as a result of harvest, but were lost or not reported. Then, to link this number to the overall number of beluga harvested across Nunavik and Sanikiluaq, we divided it by the estimated proportion of BEL-EHB ($Prop_{BE}(t)$) in the harvest (equation 20).

The age distribution observed in the sample of harvested animals ($AgeO(t)$) was linked to the vector of ages among dead animals ($AgeE(t)$) using a Dirichlet-Multinomial function:

$$AgeO(t) \sim \text{Dirichlet.multinomial}(\alpha = v_{Ag} \cdot Prop_{BE}(t)^2 \cdot AgeE(t)) \quad (24)$$

We note that the precision parameter v_{Ag} is scaled by the estimated proportion of BEL-EHB in the harvest ($Prop_{BE}(t)$), following the same rationale as described for pregnancy rates. Vector $AgeE(t)$ was calculated as:

$$AgeE(t) = \tilde{\mathbf{d}}(t) / \sum \tilde{\mathbf{d}}(t) \quad (25)$$

The proportion of females lactating in the sample of harvested beluga at time t ($N_{lac}(t)$) was linked to the proportion of females in the harvest expected to be lactating at time t ($P_{lac}(t)$), as follows:

$$N_{lac}(t) \sim \text{betabinomial}(N_{AFL}(t), \alpha, \beta) \quad (26)$$

with

$$\alpha = v_{pr} \cdot \text{Prop}_{BE}(t)^2 \cdot P_{lac}(t) \quad (27)$$

and

$$\beta = v_{pr} \cdot \text{Prop}_{BE}(t)^2 \cdot (1 - P_{lac}(t)) \quad (28)$$

where $N_{AFL}(t)$ is the observed number of adult females examined for evidence of lactation at time t , v_{pr} is the precision of pregnancy rates proportions, and $\text{Prop}_{BE}(t)$ is the estimated proportion of the sample from the BEL-EHB stock at time t . We note that $P_{lac}(t)$ accounts for harvested females with calves aged from 0 to 1 year (since 1-year-old dependent calves are still expected to be nursing). We thus calculated $P_{lac}(t)$ as the number of harvested females with newborn calves (W) at year t , plus the number of harvested available females (A) that had been W females at year $t-1$ (conditioned upon the joint probability of female survival and calf survival), divided by the total number of adult females in the harvest.

PRIORS

We used uninformative priors for most parameters, except for ρ and SnL . For ρ , which describes the relative effects of density dependence on pregnancy, we used an informative prior based on the St. Lawrence Estuary beluga population (Tinker et al. 2024). The correction factors for struck and lost in Nunavik hunts are unknown, but studies from Alaska, Nunavut, and Greenland suggest these factors range from 1.10 to 1.41 and vary spatio-temporally, depending on hunting practices, landscape and season. For instance, Innes and Stewart (2002) reported a correction factor of 1.41 from Canada and Greenland, whereas Heide-Jørgensen and Rosing-Asvid (2002) reported 1.10 and 1.30 for Greenland before 1995 and after 1995, respectively. A recent population modelling study used an average correction factor of 1.27 (Biddlecombe et al. 2024), which we adopted here. Using this correction factor (SnL_{corr}), the proportions of beluga recovered and reported ($Q = 1/SnL_{corr}$) is 0.79, and struck and lost ($SnL = 1 - Q$) is 0.21. We assumed that SnL follows a beta distribution with a mean of 0.21 and a standard error of 0.05 (alpha = 14.0, beta = 51.9). We also explored alternative scenarios where SnL_{corr} was either reduced or augmented by 10% (1.17 and 1.37) to quantify the impact of this correction factor on model-based estimates.

We also used informative priors or applied constraints on some derived parameters to facilitate convergence and ensure that the model predicted realistic outcomes. For instance, while calculating carrying capacity (K), we applied the logical constraint that at K , asymptotic population growth rate, λ , should be 1 (stable population). We used a prior for the maximum value for λ ($\lambda_{max} = \exp(R_{max})$) with a log-normal distribution centered at a mean of 1.04 ($\exp(\text{default } R_{max} \text{ for cetaceans})$) and a SD of 0.008. As a result, 95% of the prior distribution of λ_{max} fell between approximately 1.01 and 1.07, corresponding to 1% and 7% annual growth, respectively. Refer to Table 5 for the full list of priors and their corresponding values.

MODEL ANALYSIS

Model Fitting and validation

Model was coded and fitted through R version 4.4.0 (R Core Team 2024) and Stan version 2.35.0 (Carpenter et al. 2017). Parameters were estimated using Markov Chain Monte Carlo (MCMC) methods. We aimed for a posterior distribution of 10,000 samples, which was attained by using 20 chains with a thinning of 1 and a warm-up phase of 300 iterations and 500 sampling iterations per chain. We relied on a suite of methods to assess model fit and to perform model validation. First, we visually inspected the trace plots to assess the level of mixing of the chains and convergence. Then, we verified the Gelman-Rubin convergence statistic (\hat{R}), where \hat{R} below 1.1 indicated good chain mixing. We also verified that the effective number of samples (n_{eff}) was not well below the actual number of iterations (minus warm-up), which would indicate poor MCMC sampling efficiency (McElreath 2020). Further, we compared the posterior and prior distributions for all parameters to assess whether and to what extent the parameters were updated. We conducted posterior predictive checks as an evaluation of model goodness of fit. Specifically, we derived out-of-sample predictions of harvest numbers, survey abundance, and pregnancy rates. Then, we visually checked how predicted values matched with observed values for each source of data. Bayesian P-values were computed as the discrepancy between the sum of squared Pearson residuals for predicted and observed values, with $0.05 < P < 0.95$ indicating good fit to the data.

Model analysis and scenarios

We used this IPM model to estimate demographic rates, population abundance over time, the number of BEL-EHB beluga harvested annually, and the relative contribution of harvest and other sources to overall mortality. We also used the IPM to project population abundance forward in time (i.e., 1000 years) in the absence of harvest to estimate current carrying capacity, K , and maximum rate of population increase, R_{max} . Finally, we explored the impact of perturbations in struck and loss, i.e., we ran the model with three values for Snl_corr : 1) 1.17, 2) 1.27 and 3) 1.37.

Results from the new IPM were then compared to results obtained with those from the SPM (Hammill et al. 2023b; Sauvé et al. 2024) run using harvest data up to 2023. We compared model-based estimates of three parameters:

1. 2023 abundance,
2. Estimated harvest levels over the time series, and
3. Carrying capacity.

In Hammill et al. (2023b), a concern was raised about the possibility that the 2021 survey estimate was an outlier in the time series due to its very small confidence interval relative to the others. Therefore, Hammill et al. (2023b) presented two model runs; one with the variance as is and one with an augmented variance, corresponding to the average CV reported for the remainder of the time series. Here, our comparison pertains to the first model run, i.e., using the CV estimated from the 2021 survey data (St-Pierre et al. 2024).

RESULTS

POPULATION DYNAMICS UNDER THE IPM

Trace plots of all estimated parameters showed good mixing of the 20 chains. \hat{R} was below 1.1 and N_{eff} was large for all parameters (Table 6). Priors were updated for all parameters, except for ρ where the posterior distribution was similar to the (informed) prior distribution (Figure A2). Interestingly, the parameter ξ was updated and was estimated at 0.83 (95% Credible Interval, CrI = [0.56; 0.99]), suggesting that there is approximately a 17% proportional reduction in harvest hazards for lactating females relative to other adult females of the same age. This result suggests that there is a 17% avoidance of females with calves by hunters. Out-of-sample predictions matched well with observations for harvest numbers (Figure A3), survey abundance (Figure A4), and pregnancy rates (Figure A5). The age and sex structure within harvested animals estimated by the model matched well with the observations (Figure A6). The combined Bayesian p-value was 0.43 (Figure A7), which indicated good fit to the data.

The model allowed estimating age-specific variation in demographic rates over the time series. Taking year 2023 as an example, model results indicated an increasing survival probability for males up to approximately age 5, followed by a slow decline starting at age 11 (Figure 5A). A similar pattern was estimated for non-reproducing females, with an increase in survival with age up until age 5 and then a decline starting at 9 years of age (Figure 5B). After 9 years old, non-reproducing females and pregnant females showed a similar decline in age-specific survival (Figure 5B-C). Females with a calf had higher survival rates and a slower decline in survival with age, compared to other females (Figure 5D), reflecting a lower probability of being harvested as determined by the parameter ξ . Indeed, model estimate of ξ was 0.83 (95% CrI = [0.55, 0.99]), indicating a 17% reduction in harvest mortality hazards for lactating females relative to other females. The probability that a non-reproducing adult female becomes pregnant the following year was high (98%) until age 42, after which the probability of becoming pregnant declined rapidly with age (Figure 5E).

Over the time series (1974-2023), the model estimated several fluctuations in survival rates, although there is a high degree of uncertainty associated with the estimates. Survival of calves and yearlings both showed signs of increase (Figure 6A), although there was considerable uncertainty around these trends. Calf survival ranged from 0.55 (95% CrI = [0.36, 0.71]) in 1974 to 0.72 (95% CrI = [0.58, 0.82]) in 2009. Yearling survival ranged from 0.77 (95% CrI = [0.67, 0.85]) in 1974 to 0.86 (95% CrI = [0.80, 0.91]) in 2023 (Figure 6B). For juveniles (e.g., 5 year-olds; Figure 6C), the model predicted an initial increase in survival between years 1974 and 1981, and then a stabilization at around 0.94 (95% CrI = [0.92, 0.96]) afterwards. Patterns in survival probabilities were similar for adult males and females, with the model suggesting an increase between 1980 and 1986, then a plateau between approximately 1986 and 2009 and finally a slight decreasing trend afterwards. The 2023 estimate of 8 years-old survival was 0.95 (95% CrI = [0.93, 0.96]; Figure 6D) for males and 0.94 (95% CrI = [0.93, 0.95]; Figure 6D) for females. Over the time series, the probability that a non-reproducing female becomes pregnant remained stable (Figure 6E), with the 2023 estimate being 0.97 (95% CrI = [0.71, 1.00]) in 2023; however, there were large uncertainties around these estimates.

We estimated the annual number of BEL-EHB beluga landed across Nunavik (referred to as BEL-EHB landings) by multiplying the model-derived annual BEL-EHB harvest levels by the proportion of beluga recovered and reported (Q). This estimate reflects the BEL-EHB contribution to the total harvests reported by Nunavik hunters. While similar to estimates based on harvest reports and the proportion of BEL-EHB beluga from genetic analyses (used as model input), it is updated by the model, which integrates all input data and accounts for stock dynamics. The estimated overall and BEL-EHB landings across Nunavik varied similarly over

time, especially during the first half of the time series (Figure 7). Early in the time series, the model predicted the highest landings across Nunavik and for the BEL-EHB stock, followed by a period of relatively stable landings. Across Nunavik, total landings increased around 2009, but the model did not predict a similar increase in BEL-EHB landings. The 2023 estimate is 119 (95% CrI = [106, 135]) BEL-EHB beluga landed.

Management objectives for BEL-EHB beluga have evolved over the time series, and harvest levels compatible with these management objectives have been calculated annually since 1996. Since then, estimated BEL-EHB landings have been above the harvest level compatible with the management objective for the stock 26 years out of 28. The model estimated that annual BEL-EHB beluga landings exceeded the harvest level compatible with the management objective for the stock by 42 individuals on average. The contribution of harvest to overall mortality was high throughout the time series (Figure 8), ranging between 18.9% (95% CrI = [13.0%, 26.6%]) in 2006 and 43.4% (95% CrI = [33.9%, 53.7%]) in 1980. In recent years, the proportion of mortality attributable to harvest has reached levels unobserved since the 1970s (Figure 8).

Model-based estimates of BEL-EHB abundance showed a continuous decline since the 1970s (Figure 9), with the 2023 abundance being estimated at 3,600 (95% CrI = [3,000, 4,200], rounded to the nearest 100) beluga. Since 1974, average rate of stock decline was 1.95% (95% CI = [1.52, 2.40]) annually, and over the last ten years (2014-2023), this rate of decline reached an average of 2.24% (95% CI = [1.20, 3.44]) annually.

To estimate current carrying capacity, we projected the model forward in time in the absence of harvest mortality, and assuming future environmental conditions (through environmental stochasticity parameter) are similar to those observed over the time series. Carrying capacity was estimated at 10,100 (95%CrI = [8,500, 12,200], rounded to the nearest 100) animals. In the absence of harvesting, the maximum theoretical rate of population increase was 3.35% (95% CrI = [2.18%, 4.50%]).

Varying the rate of struck and lost affected the intercept of population abundance and increased the relative contribution of harvest to overall mortality (Figure 10). Specifically, when struck and lost correction factor increased from 1.17 to 1.37, the relative contribution of harvest to overall mortality increased slightly from an average of 29% to 31% across the time series and the estimated population abundance also increased, especially earlier in the time series. For example in 1974, the estimated population size was 9,000 and 9,500 (rounded to the nearest 100) using a struck and lost correction factor of 1.17 and 1.37, respectively.

COMPARISON BETWEEN IPM AND SPM

Compared with the SPM, the IPM estimated a similar trend between 1974 and approximately 2010, after which the IPM predicted a slower population decline (Figure 11). Of particular notice is the much reduced uncertainties around abundance estimated by the IPM. The 2023 estimate of BEL-EHB abundance using the SPM was 2,600 (95% CrI = [1,100; 4,200], rounded to the nearest 100) beluga. Since 1974, SPM predicted that the median rate of stock decline was 2.38% (95% CI = [0.06, 4.90] vs. 1.95 with 95% CI = [1.52, 2.40] for the IPM) annually, and over the last ten years (2014-2023), this rate of decline reached a median of 3.82% (95% CI = [-2.17, 11.54]; vs. 2.24% with 95% CI = [1.20, 3.44] for the IPM) annually. The SPM and the IPM yielded similar predictions of the number of BEL-EHB beluga landed each year (Figure 12). According to the SPM, the 2023 estimate is 187 BEL-EHB beluga landed, compared to 119 for the IPM. Under the SPM, the number of BEL-EHB beluga landed each year was above the harvest level compatible with the management objective for the stock in 100% of the years and exceeded it by 72 individuals on average. The SPM predicted K to be 11,000 (95%CrI = [6,400,

19,400], rounded to the nearest 100), which overlaps with the estimates from the IPM considerably (10,100; 95%CrI = [8,500, 12,200]).

DISCUSSION

The integrated population model presented here builds upon insights and methods from previous quantitative analyses of the BEL-EHB beluga stock (e.g., Hammill et al. 2023b; Sauvé et al. 2024). However, the IPM incorporates many additions, including the use of new sources of information: age and sex composition of the harvest, pregnancy rates calculated from progesterone analysis of blubber samples and lactation status derived from necropsies performed on harvested beluga. By including information on age and sex composition of the harvest, we were able to improve our process model to better account for age- and sex-specific demographic rates. This provided insights into age- and sex-specific trends in BEL-EHB beluga survival, information that could not be estimated from the SPM. Measuring progesterone levels from blubber samples collected from Nunavik beluga also allowed for the estimation of pregnancy rates for this region, rather than relying on estimates reported elsewhere. In addition, the hazards formulation allowed for greater insights into the relative contributions of harvesting and other sources of mortality in BEL-EHB beluga. Further, the inclusion of annual stochasticity in the IPM provided a more realistic picture of annual fluctuations in abundance and the basis for testing and considering the effects of potential environmental factors on vital rates in future developments of the BEL-EHB beluga IPM. In the context of the rapid climate warming in the Nunavik area (Brand et al. 2014), as well as the forecasted increase in vessel traffic in the migration areas of BEL-EHB beluga (DFO 2012), understanding how threats other than subsistence harvest (e.g. food availability) could affect BEL-EHB beluga represents a priority identified by DFO (Sauvé et al. 2024) and its co-management partners (NMRWB 2024).

Overall, the IPM predicted similar population trends and abundances when compared to the SPM; however, there are a few notable differences. First, uncertainties around model-based predictions of abundance were much lower under the IPM compared to the SPM. For example, the CV around the population abundance in 2023 was 0.10 for the IPM and 0.30 for the SPM. This is likely due to the fact that the IPM bases its estimate of population abundance on multiple sources of information jointly. In contrast, the SPM solely relies on information from harvest levels and population surveys. Uncertainties associated with survey estimates are large and accordingly, the resulting abundance estimates from the SPM are also large. Second, the recent BEL-EHB abundance estimated by the IPM (3,600; 95% CrI = [3,000, 4,200]) is higher than the SPM estimate (2,600 with 95% CrI = [1,100; 4,200]), and the point estimate of the rate of decline between 2014 and 2023 is lower in the IPM (2.24% with 95% CI = [1.20, 3.44], compared to 3.82% with 95% CI = [-2.17, 11.54] in the SPM). The incorporation of other data sources therefore also appeared to reduce the relative influence of the most recent aerial survey abundance estimate from 2021 – the lowest in the time series and with the smallest confidence interval (St-Pierre et al. 2024) - on the demographic model abundance estimates and trend. Similarly, increasing the variance associated with this 2021 aerial survey abundance estimate yielded a slower population rate of decline in the SPM (Hammill et al., 2023b), further demonstrating the major influence of this source of data in the SPM. A new BEL-EHB aerial survey was flown in summer 2024, which will provide additional information that should contribute to ascertaining the recent demographic trend of the BEL-EHB stock. Finally, estimated annual BEL-EHB landings by the IPM were smaller than those estimated by the SPM, especially early in the time series. Again, this can be explained by the SPM matching the low 2021 aerial survey estimate more closely than the IPM due to fewer sources of data informing the SPM. Achieving such a low population size in 2021 requires the SPM to estimate higher harvest levels throughout the time series.

The data on the age and sex structure of BEL-EHB beluga, along with female reproductive rates incorporated into the IPM, is derived from samples provided by Nunavik hunters. While beluga harvested in eastern Hudson Bay during July and August are, by definition, BEL-EHB beluga, those harvested in other seasons and areas of the Nunavik coastline represent a mix of BEL-EHB, WHB, JB and Cumberland Sound populations or stocks (Turgeon et al. 2009; Parent et al. 2023). The proportion of individuals from each population or stock in the total beluga harvest per management area and season are estimated using a Genetic Mixture Analysis model (GMA; Parent et al. (2023). Unlike individual assignment methods, the GMA does not assign each individual to a specific population or stock. Instead, it takes into account the probability of each individual sample belonging to the different reference populations. Individual genetic assignments for the BEL-EHB reference group are highly uncertain with the currently available mitochondrial DNA markers (Parent et al. 2024). Consequently, we could not distinguish BEL-EHB samples from non-BEL-EHB ones, and we used samples from all beluga harvested along the Nunavik coastline to inform our IPM on age and sex structure, as well as annual reproductive rates. This information is therefore not specific to BEL-EHB beluga. The BEL-EHB stock is relatively small compared to the WHB stock (estimated at 54,500 beluga in 2015; Matthews et al. 2017), and faces considerable subsistence harvest pressure. Harvesting, by increasing mortality, can impose selective pressures on wildlife populations and alter reproductive schedules and population structure (Mysterud 2011). It is thus possible that the sex and age structure, as well as life-history traits of BEL-EHB beluga differ from other stocks harvested by Nunavik hunters (e.g., Lesage et al. 2001, 2009). Being able to specifically target samples from the BEL-EHB stock to inform our demographic model would yield better predictions of the dynamics of this particular stock. This could potentially be achieved by determining the genetic origin of each beluga individually through analyses of nuclear DNA. Further advancements in beluga genetics are needed to identify the stock of origin of a given sample collected outside of summering grounds (Parent et al. 2024).

The beluga age data used as input in our IPM was estimated from dental analysis, which consists of counting growth layer groups in the dentine of a longitudinal midline section of a tooth. Yet, in old beluga and particularly for animals aged 34 years or older, tooth wear and reduced growth can lead to age underestimation (Sergeant 1973; Lesage et al. 2014). This can lead to an overrepresentation of middle-aged beluga in the population and an overestimation of mortality for older age classes. Although animals aged 40 years or older appear less frequent in our samples (Figure 3), those aged > 75 years are represented in the age structure, indicating that dental analysis can identify at least a proportion of older individuals sampled. Quantitative evidence is lacking to inform any correction factor that would assign a proportion of middle-aged animals to older age classes, thus such a correction has not been used in our IPM. In the future, simulations assessing the effect of underestimating the age of various proportions of the older animals from our samples on the demographic dynamics of the BEL-EHB stock could provide information on the potential implications of the aging method used for beluga.

In parametrizing the model, some assumptions had to be made when information was not available. First, sample size in the reproductive dataset was too small to yield information on age-specific pregnancy rates. We assumed that females start reproducing at 8 years of age, but this assumption could be challenged. Due to limited sample size, the data on pregnancy rates currently has a lower contribution to the model compared to other sources of data (Figure A8). As samples continue to be collected in the future, the importance of this dataset is likely to increase and it may become possible to obtain age-specific pregnancy rates and revisit our assumption regarding age at first reproduction.

Second, the age structure derived from samples provided by hunters was right-skewed (i.e., younger animals were greatly under-represented, with the youngest age classes almost

entirely absent). Demographic changes such as a decline in birth rates, increased longevity, and higher juvenile dispersal could explain a right-skewed age structure to some degree. However, the degree of age-bias was greater than could be explained by any feasible demographic schedule, and we thus assumed that the observed underrepresentation of younger age classes in our data represented an artifact of harvesting and/or sampling rather than a characteristic of the BEL-EHB stock. Such a bias could reflect various factors, including preferences for larger, white beluga by harvesters, or the use of different age-specific migration paths resulting in reduced probability for hunters to encounter younger animals along the Nunavik coastline. We also assumed that the observed age structure was representative of the beluga harvested in the Nunavik region, i.e., that there was no systematic bias in the age of beluga sampled and submitted by hunters. To better understand what could explain this under-representation of younger individuals in our sample, we consulted the Anguvigait and Anguvigaq managers and presidents. They unanimously indicated that hunters preferentially harvest larger beluga and do not select which of the catches they sample based on the size, color or age of the animal, indicating that the observed age structure is reflective of beluga harvested in Nunavik.

Third, we calculated the proportion of BEL-EHB beluga in the Nunavik harvest using the genetic composition outlined in the most recent analysis (Parent et al. 2023). These proportions were determined by season and management area, using all samples collected over the last four decades. This approach assumes that the genetic composition of the harvest has remained consistent throughout the time series. However, in the context of a declining BEL-EHB stock, and stable or increasing trends in other stocks, one might reasonably conclude that the proportion of BEL-EHB beluga in the Nunavik harvest could have decreased over time. Alternatively, if migratory routes used by BEL-EHB beluga are consistently closer to the coastline compared to that of other stocks, the composition of the harvest might display minimal variation despite changes in stock abundance. This is supported by the high percentages of BEL-EHB observed in the harvest – up to 50% in northeast Hudson Bay and 40% in Hudson Strait during the fall – compared to the expected 5% based on relative abundances of the BEL-EHB and WHB stocks, assuming both stocks are equally available to hunters during migration. Examining trends in the stock composition of the Nunavik beluga harvest over recent decades could provide valuable insights into potential density-dependent effects on the susceptibility of BEL-EHB beluga to harvesting.

In the SPM, harvest represents the only source of annual variation in mortality for BEL-EHB beluga. The SPM therefore adjusts the historic population estimate and the parameters of the productivity model of the stock to fit the observed abundance estimates and the harvest levels through the entire time period of interest. In the IPM, harvest hazards represent one of two distinct sources of mortality, the other being mortality due to all other causes combined (e.g., predation, diseases). This allows estimating the relative contribution of harvest to overall mortality. With the current model parametrization, harvest-induced mortality accounted for 19 to 43% of total mortality, and this proportion has increased in recent years. While this suggests that harvests represent one of the most important sources of mortality for BEL-EHB beluga, the contribution of harvest to overall mortality is sensitive to the value of struck and loss used. Moreover, running the model with struck and lost correction factors of 1.17 and 1.37 shows that higher struck and lost rates imply a greater overall population size, especially earlier in the time series. This can be explained by the model adjusting initial population size to sustain a higher harvest rate across the time series while being constrained by other sources of information indicating a certain rate of decline.

In both the IPM and the SPM, the struck and lost parameter encompassed all beluga mortalities associated with harvest activities that are unaccounted for in the harvest numbers reported, including non-recovery and non-reporting. There is currently very little data available to directly

inform the model on either source of bias for BEL-EHB beluga. To account for uncertainty in this parameter we used a beta distribution with a mean of 21% based on the previous BEL-EHB stock assessments and insights from other beluga stocks (Hammill et al. 2023b; Richard, 2008; Biddlecombe et al. 2024). We also assumed the struck and lost parameter to be constant over the time series and among management areas, as in previous BEL-EHB beluga stock assessments (e.g., Hammill et al. 2017; Hammill et al. 2023b). However, hunting practices may differ between management areas and may have changed over time. Also, knowledge holders indicate that compliance with reporting of harvests has varied over the last decades depending on the management measures in place. The value used for struck and lost has an impact on abundance estimates and the relative contribution of harvests to overall mortality. Given the increasing interest by co-management partners to estimate and mitigate mortality in BEL-EHB beluga associated with threats other than harvesting (NMRWB 2024), and the need for information on struck and lost to quantify the contribution of other threats to BEL-EHB beluga mortality, efforts should be made to improve estimates for this parameter for the BEL-EHB beluga stock. Focused workshops with elders and hunters to gather information about their evaluation of rates of recovery during the harvest and non-reporting, as well as how those sources of struck and lost might have changed over time, e.g. in relation to changes in hunting practices or management measures in place would therefore be essential to further explore temporal dynamics in BEL-EHB beluga mortality.

In summary, the IPM proposed in this study performed as expected, and our results indicate that BEL-EHB stock abundances and trends generally agree with those predicted by the SPM used in previous stock assessments. This is partly because of the large uncertainties around SPM-based estimates. The IPM provided greater precision and yielded different point estimates of population size and rate of population decline, which should impact model-based projections in the future and harvest advices. Further, the IPM allows for insights that were not possible with the SPM: these improvements were possible because of the addition of key life-history data from the samples provided by Nunavik and Sanikiluaq beluga hunters. The IPM allowed us to estimate the non-harvest-induced component of mortality, and provided greater insights into the demographic processes being modelled – a key characteristic of IPMs (Besbeas et al. 2005; Schaub and Abadi 2011). In addition, the structure of the IPM aligns with that of demographic models recently developed and implemented for marine mammal stock assessments in eastern Canada (Hammill, et al. 2023b; Tinker et al. 2023, 2024). We have highlighted specific additional information that would improve the parametrization of the IPM. Future sampling and data collection efforts should focus on these topics to tackle the main sources of uncertainties identified for BEL-EHB beluga demographic modelling and for DFO to address the priorities identified by its co-management partners and resource users.

REFERENCES CITED

- Bailleul, F., Lesage, V., Power, M., Doidge, D.W., and Hammill, M.O. 2012a. Differences in diving and movement patterns of two groups of beluga whales in a changing Arctic environment reveal discrete populations. *Endanger. Species Res.* 17: 27–41.
- Bailleul, F., Lesage, V., Power, M., Doidge, D.W., and Hammill, M.O. 2012b. Migration phenology of beluga whales in a changing Arctic. *Clim. Res.* 53: 169–178.
- Besbeas, P., Freeman, S.N., and Morgan, B.J.T. 2005. The potential of integrated population modelling. *Aust. N. Z. J. Stat.* 47: 35–48.
- Biddlecombe, B.A., and Watt, C.A. 2024. Modeling population dynamics of beluga whales in the Eastern High Arctic – Baffin Bay population. *J. Wild. Manag.* 88:e22657.
- Brand, U., Came, R.E., Affek, H., Azmy, K., Mooi, R., and Layton, K. 2014. Climate-forced change in Hudson Bay seawater composition and temperature, Arctic Canada. *Chem. Geol.* 388: 78–86.
- Brennin, R., Murray, B.W., Friesen, M.K., Maiers, L.D., Clayton, J.W., and White, B.N. 1997. Population genetic structure of beluga whales (*Delphinapterus leucas*): mitochondrial DNA sequence variation within and among North American populations. *Can. J. Zool.* 75: 795–802.
- Breton-Honeyman, K., Hammill, M.O., Furgal, C.M., and Hickie, B. 2016. Inuit knowledge of beluga whale (*Delphinapterus leucas*) foraging ecology in nunavik (Arctic Quebec), Canada. *Can. J. Zool.* 94: 713–726.
- Brown Gladden, J.G., Ferguson, M.M., and Clayton, J.W. 1997. Matriarchal genetic population structure of North American beluga whales *Delphinapterus leucas* (Cetacea: Monodontidae). *Mol. Ecol.* 6: 1033–1046.
- Brown Gladden, J.G., Ferguson, M.M., Friesen, M.K., and Clayton, J.W. 1999. Population structure of North American beluga whales (*Delphinapterus leucas*) based on nuclear DNA microsatellite variation and contrasted with the population structure revealed by mitochondrial DNA variation. *Mol. Ecol.* 8: 347–363.
- Burns, J.J., and Seaman, G.A. 1986. Investigations of belukha whales in coastal waters of western and northern Alaska. II. Biology and ecology. US Department of Commerce, NOAA, OCSEAP Final Report 56:221–357.
- Caron, L.M.J., and Smith, T.G. 1990. Philopatry and site tenacity of belugas, *Delphinapterus leucas*, hunted by the Inuit at the Nastapoka estuary, eastern Hudson Bay. *Can. Bull. Fish. Aquat. Sci.* 224 :69–79.
- Carpenter, B., Gelman, A., Hoffman, M.D., Lee, D., Goodrich, B., Betancourt, M., Brubaker, M., Guo, J., Li, P., and Riddell, A. 2017. Stan: A probabilistic programming language. *J. Stat. Softw.* 76:32.
- Caswell, H., de Vries, C., Hartemink, N., Roth, G., and van Daalen, S.F. 2018. Age × stage-classified demographic analysis: a comprehensive approach. *Ecol. Monogr.* 88: 560–584.
- Colbeck, G.J., Duchesne, P., Postma, L.D., Lesage, V., Hammill, M.O., and Turgeon, J. 2013. Groups of related belugas (*Delphinapterus leucas*) travel together during their seasonal migrations in and around Hudson Bay. *Proc. R. Soc. B.* 280: 20122552.
- COSEWIC. 2016. Special Report Designatable Units for Beluga Whales (*Delphinapterus leucas*) in Canada. Committee on the Status of Endangered Wildlife in Canada, 73 p.

-
- COSEWIC. 2020. COSEWIC assessment and status report on the Beluga Whale *Delphinapterus leucas*, Eastern High Arctic - Baffin Bay population, Cumberland Sound population, Ungava Bay population, Western Hudson Bay population, Eastern Hudson Bay population and James Bay population in Canada. Committee on the Status of Endangered Wildlife in Canada, xxxv + 84.
- DFO. 2012. Science review of Baffinland's Mary River Project final environmental impact statement. Can. Sci. Advis. Sec. Sci. Advis. Rep. 2012/016.
- DFO and NMRWB. 2021. Beluga management system-regional rules in the Nunavik marine region.
- Dodge, D. W. 1990b. Age and stage based analysis of the population dynamics of beluga whales, *Delphinapterus leucas*, with particular reference to the northern Quebec population. PhD Dissertation. *McGill University*, 190 p.
- Eberhardt, L.L. 2002. A paradigm for population analysis of long-lived vertebrates. *Ecology* 83: 2841–2854.
- Ellis, S., Franks, D.W., Natrass, S., Currie, T.E., Cant, M.A., Giles, D., Balcomb, K.C., and Croft, D.P. 2018. Analyses of ovarian activity reveal repeated evolution of post-reproductive lifespans in toothed whales. *Sci. Rep.* 8: 12833.
- Ferguson, S.H., Willing, C., Kelley, T.C., Boguski, D.A., Yurkowski, D.J., and Watt, C.A. 2020. Reproductive parameters for female beluga whales (*Delphinapterus leucas*) of Baffin Bay and Hudson Bay, Canada. *Arctic*. 73: 405–420.
- Finley, K. J., Miller, G. W., Allard, M., Davis, R. A., and Evans, C. R. 1982. The belugas (*Delphinapterus leucas*) of northern Quebec: distribution, abundance, stock identity, catch history and management. *Can. Tech. Rep. Fish. Aquat. Sci.* 1123: vi + 57.
- Goertz, C.E.C., Burek-Huntington, K., Royer, K., Quakenbush, L., Clauss, T., Hobbs, R., and Kellar, N.M. 2019. Comparing progesterone in blubber and serum to assess pregnancy in wild beluga whales (*Delphinapterus leucas*). *Conserv. Physiol.* 7 : 10.1093.
- Gosselin, J.-F., Hammill, M.O., and Mosnier, A. 2017. Indices of abundance for beluga (*Delphinapterus leucas*) in James Bay and eastern Hudson Bay in summer 2015. *DFO Can. Sci. Advis. Sec. Res. Doc.* 2017/067. iv + 25 p.
- Hammill, M.O., Mosnier, A., Gosselin, J.-F., Matthews, C.J.D., Marcoux, M., and Ferguson, S.H. 2017. Management approaches, abundance indices and total allowable harvest levels of belugas in Hudson Bay. *DFO Can. Sci. Advis. Sec. Res. Doc.* 2017/062. iv + 43 p.
- Hammill, M.O., Rossi, S.P., Mosnier, A., den Heyer, C.E., Bowen, W.D., and Stenson, G.B. 2023a. Grey seal abundance in Canadian waters and harvest advice. *DFO Can. Sci. Advis. Sec. Res. Doc.* 2023/053. iv + 40 p.
- Hammill, M.O., St-Pierre, A.P., Mosnier, A., Parent, G.J., and Gosselin, J.-F. 2023. Total Abundance and Harvest Impacts on Eastern Hudson Bay and James Bay Beluga 2015–2022. *DFO Can. Sci. Advis. Sec. Res. Doc.* 2023/066. iv + 50 p.
- Heide-Jørgensen, M.P., and Rosing-Asvid, A. 2002. Catch statistics for beluga in West Greenland 1862 to 1999. *NAMMCO Scientific Publications* 4: 127–142.
- Heide-Jørgensen, M.P., and Teilmann, J. 1994. Growth, reproduction, age structure and feeding habits of white whales (*Delphinapterus leucas*) in West Greenland waters. *Meddelelser om Grønland, Bioscience*. 39: 195–212.
-

-
- Hobbs, R.C., Reeves, R.R., Prewitt, J. S., Desportes, G., Breton-Honeyman, K., Christensen, T., Citta, J.J., et al. 2016. Global review of the conservation status of Monodontid stocks. *Mar. Fish. Rev.* 81:1-53.
- Hobbs, R.C., Wade, P.R., and Shelden, K.E.W. 2015. Viability of a small, geographically-isolated population of beluga whales, *Delphinapterus leucas*: effects of hunting, predation, and mortality events in Cook Inlet, Alaska. *Mar. Fish. Rev.* 77: 59–88.
- Innes, S., and Stewart, R.E.A. 2002. Population size and yield of Baffin Bay beluga (*Delphinapterus leucas*) stocks. NAMMCO Scientific Publications. 4: 225–238.
- Lair, S., Measures, L.N., and Martineau, D. 2015. Pathologic findings and trends in mortality in the beluga (*Delphinapterus leucas*) population of the St Lawrence Estuary, Quebec, Canada, from 1983 to 2012. *Vet. Pathol.* 53: 1–15.
- Lemire, M., Kwan, M., Laouan-Sidi, A.E., Muckle, G., Pirkle, C., Ayotte, P., and Dewailly, E. 2015. Local country food sources of methylmercury, selenium and omega-3 fatty acids in Nunavik, Northern Quebec. *Sci. Total Environ.* 509–510: 248–259.
- Lesage, V. Baillargeon, D., Turgeon, S. and Doidge, DW. 2009. Harvest statistics for beluga in Nunavik, 2005–2008. DFO Can. Sci. Advis. Sec. Res. Doc. 2009/007. iv + 21 p.
- Lesage, V. Doidge, D.W., and Fibich, R. 2001. Harvest statistics for beluga whales in Nunavik, 1974–2000. DFO Can. Sci. Advis. Sec. Res. Doc. 2001/022. iv + 35 p.
- Lesage, V., Measures, L.N., Mosnier, A., Lair, S., Michaud, R., and Béland, P. 2014. Mortality patterns in St. Lawrence Estuary beluga (*Delphinapterus leucas*), inferred from the carcass recovery data, 1983–2012. DFO Can. Sci. Advis. Sec. Res. Doc. 2013/118. iv + 23 p.
- Lewis, A.E., Hammill, M.O., Power, M., Doidge, D.W., and Lesage, V. 2009. Movement and aggregation of eastern Hudson Bay beluga whales (*Delphinapterus leucas*): a comparison of patterns found through satellite telemetry and Nunavik traditional ecological knowledge. *Arctic.* 62: 13–24.
- de March, B.G.E., Maiers, L.D., and Friesen, M.K. 2002. An overview of genetic relationships of Canadian and adjacent populations of belugas (*Delphinapterus leucas*) with emphasis on Baffin Bay and Canadian eastern Arctic populations. NAMMCO Scientific Publications. 4: 17–38.
- de March, B.G.E., and Postma, L.D. 2003. Molecular genetic stock discrimination of belugas (*Delphinapterus leucas*) hunted in eastern Hudson Bay, Northern Quebec, Hudson Strait, and Sanikiluaq (Belcher Islands), Canada, and comparisons to adjacent populations. *Arctic.* 56: 111–124.
- de March, B.G.E., Stern, G.A., and Innes, S. 2004. The combined use of organochlorine contaminant profiles and molecular genetics for stock discrimination of white whales (*Delphinapterus leucas*) hunted in three communities on southeast Baffin Island. *J. Cetac. Res. Manage.* 6: 241–250.
- Matthews, C.J.D., and Ferguson, S.H. 2015. Weaning age variation in beluga whales (*Delphinapterus leucas*). *J Mammal.* 96: 425–437.
- Matthews, C.J.D., Watt, C.A., Asselin, N.C., Dunn, J.B., Young, B.G., Montsion, L.M., Westdal, K.H., Hall, P.A., Orr, J.R., Ferguson, S.H., and Marcoux, M. 2017. Estimated abundance of the Western Hudson Bay beluga stock from the 2015 visual and photographic aerial survey. DFO Can. Sci. Advis. Sec. Res. Doc. 2017/061. v + 20 p.
-

-
- McAlpine, D.F., Kingsley, M.C.S., and Daoust, P.-Y. 1999. A lactating record-age St. Lawrence Beluga (*Delphinapterus leucas*). *Mar. Mamm. Sci.* 15: 859–863.
- McElreath, R. 2020. Statistical rethinking: a Bayesian course with examples in R and Stan. CRC Press, Boca Raton, FL. 459 p.
- Mosnier, A., Doniol-Valcroze, T., Gosselin, J.F., Lesage, V., Measures, L.N., and Hammill, M.O. 2015. Insights into processes of population decline using an integrated population model: the case of the St. Lawrence Estuary beluga (*Delphinapterus leucas*). *Ecol. Modell.* 314: 15–31. Elsevier.
- Mysterud, A. 2011. Selective harvesting of large mammals: How often does it result in directional selection? *J. Appl. Ecol.* 48: 827–834.
- NAMMCO. 2018. Global Review of Monodontids. North Atlantic Marine Mammal Commission Report, Hillerød, Denmark, 277.
- NMRWB. 2024. Regular public meeting #63 meeting minutes.
- Parent, G.J., Montana, L., Bonnet, C., Parent, É., St-Pierre, A.P., Watt, C., and Hammill, M.O. 2024. Genetic monitoring program for beluga (*Delphinapterus leucas*) harvested in the Nunavik and Nunavut (Belcher Islands) regions. *Can. Tech. Rep. Fish. Aquat. Sci.* 0000: v+xp.
- Parent, G.J., Mosnier, A., Montana, L., Cortial, G., St-Pierre, A.P., Bordeleau, X., Lesage, V., Watt, C., Postma, L., and Hammill, M.O. 2023. Re-examining populations of beluga in the Hudson Bay Strait Complex and assessing the impact on harvests in Nunavik and Sanikiluaq management units. *DFO Can. Sci. Advis. Sec. Res. Doc.* 2023/004: iv + 31 p.
- Postma, L.D. 2017. Genetic diversity, population structure and phylogeography among belugas (*Delphinapterus leucas*) in Canadian waters: broad to fine-scale approaches to inform conservation and management strategies. PhD dissertation. University of Manitoba. 314 p.
- Postma, L.D., Petersen, S.D., Turgeon, J., Hammill, M.O., Lesage, V., and Doniol-Valcroze, T. 2012. Beluga whales in James bay a separate entity from eastern hudson bay belugas. *DFO Can. Sci. Advis. Sec. Res. Doc.* 2012/074.iii + 23 p.
- R Core Team. 2024. R: a language and environment for statistical computing. R Foundation for Statistical Computing, Vienna, Austria.
- Reeves, R.R., and Mitchell, E. 1987. History of white whale (*Delphinapterus leucas*): exploitation in eastern Hudson Bay and James Bay. *Can. Spec. Publ. Fish. Aquat. Sci.* 95: 45 p.
- Renaud, L.A., Bordeleau, X., Kellar, N.M., Pigeon, G., Michaud, R., Morin, Y., Lair, S., Therien, A., and Lesage, V. 2023. Estimating pregnancy rate from blubber progesterone levels of a blindly biopsied beluga population poses methodological, analytical and statistical challenges. *Conserv. Physiol.* 11: 10.1093.
- Richard, P.R. 2008. On determining the Total Allowable Catch for Nunavut odontocete stocks. *Can. Sci. Advis. Sec. Res. Doc.* 2008/022. iii + 12 p.
- Richard, P.R. 2010. Stock definition of belugas and narwhals in Nunavut. *DFO Can. Sci. Advis. Sec. Res. Doc.* 2010/022. iv + 14.
- Rioux, È., Lesage, V., Postma, L.D., Pelletier, É., Turgeon, J., Stewart, R.E.A., Stern, G., and Hammill, M.O. 2012. Use of stable isotopes and trace elements to determine harvest composition and wintering assemblages of belugas at a contemporary ecological scale. *Endanger. Species Res.* 18, 179–191.

-
- Roth, G., and Caswell, H. 2016. Hyperstate matrix models: extending demographic state spaces to higher dimensions. *Methods Ecol. Evol.* 7: 1438–1450.
- Sauvé, C., Caissy, P., Hammill, M.O., Mosnier, A., St-Pierre, A.P., and Gosselin, J.-F. 2024. Recovery potential assessment for beluga (*Delphinapterus leucas*) stocks in Nunavik (Northern Quebec). DFO Can. Sci. Advis. Sec. Res. Doc. 2024/030. v + 70 p.
- Schaub, M., and Abadi, F. 2011. Integrated population models: a novel analysis framework for deeper insights into population dynamics. *J. Ornithol.* 152: S227–S237.
- Seaman, G.A., and Burns, J.J. 1981. Preliminary results of recent studies of belukhas in Alaskan waters. *Rep. Int. Whal. Commn.* 31: 567–574.
- Sergeant, D.E. 1973. Biology of white whales (*Delphinapterus leucas*) in Western Hudson Bay. *J. Fish. Res. Board Can.* 30: 1065–1090.
- Smith, T.G., and Hammill, M.O. 1986. Population estimates of white whale, *Delphinapterus leucas*, in James Bay, eastern Hudson Bay, and Ungava Bay. *Can. J. Fish. Aquat. Sci.* 43: 1982–1987.
- St-Pierre, A.P., Gosselin, J.-F., Mosnier, A., Sauvé, C., and Hammill, M.O. 2024. Abundance estimates for beluga (*Delphinapterus leucas*) in James Bay and the Belcher Islands-eastern Hudson Bay area in summer 2021. DFO Can. Sci. Advis. Sec. Res. Doc. 2023/040. iv + 37 p.
- Suydam, R. S. 2009. Age, growth, reproduction, and movements of beluga whales (*Delphinapterus leucas*) from the eastern Chukchi Sea. PhD dissertation. University of Washington. xi + 152.
- Tinker, T.M., Mosnier, A., St-Pierre, A.P., Gosselin, J.-F., Lair, S., Michaud, R., and Lesage, V. 2024. An integrated population model for St. Lawrence estuary belugas (*Delphinapterus leucas*). DFO Can. Sci. Advis. Sec. Res. Doc. 2023/047. iv + 61 p.
- Tinker, M.T., Stenson, G.B., Mosnier, A., and Hammill, M.O. 2023. Estimating abundance of Northwest Atlantic harp seal using a Bayesian modelling approach. DFO Can. Sci. Advis. Sec. Res. Doc. 2023/068. iv + 56 p.
- Turgeon, J., Duchesne, P., Colbeck, G.J., Postma, L.D., and Hammill, M.O. 2012. Spatiotemporal segregation among summer stocks of beluga (*Delphinapterus leucas*) despite nuclear gene flow: implication for the endangered belugas in eastern Hudson Bay (Canada). *Conserv. Genet.* 13: 419–433.
- Turgeon, J., Duchesne, P., Postma, L.D., and Hammill, M.O. 2009. Spatiotemporal distribution of beluga stocks (*Delphinapterus leucas*) in and around Hudson Bay: genetic mixture analysis based on mtDNA haplotypes. DFO Can. Sci. Advis. Sec. Res. Doc. 2009/011. iv + 14 p.
- Tyrrell, M. 2007. Sentient beings and wildlife resources: Inuit, beluga whales and management regimes in the Canadian Arctic. *Hum. Ecol.* 35: 575–586.
- Tyrrell, M. 2008. Nunavik Inuit perspectives on beluga whale management in the Canadian Arctic. *Hum. Organ.* 67: 322–334.
-

TABLES

Table 1. Aerial survey estimates of BEL-EHB beluga population size (from St-Pierre et al. 2024).

Year	Mean abundance	Standard deviation	Lower 95% CI	Upper 95% CI
1985	6,711	1,936	3,856	11,680
1993	4,163	1,760	1,880	9,217
2001	4,570	2,265	1,824	11,451
2004	7,368	2,899	3,503	15,499
2008	4,764	1,404	2,706	8,387
2011	5,001	2,350	2,084	12,002
2015	7,841	3,687	3,265	18,829
2021	2,501	719	1,440	4,345

Table 2. Pregnancy rates of beluga harvested along the Nunavik coast between October and May, 2010-2022, estimated from blubber progesterone levels.

Year	Sample size	Number of pregnant females	Proportion of pregnant females	Variance
2010	2	2	1.00	0.00
2011	2	1	0.50	0.25
2012	2	2	1.00	0.00
2013	4	2	0.50	0.25
2014	0	-	-	-
2015	2	0	0.00	0.00
2016	6	4	0.67	0.22
2017	2	0	0.00	0.00
2018	30	11	0.37	0.23
2019	28	8	0.29	0.20
2020	7	0	0.00	0.00
2021	20	7	0.35	0.23
2022	13	5	0.38	0.24

Table 3. Reported harvest of beluga in four management areas in Nunavik and in Sanikiluaq (SAN, Nunavut) from 1974-2023. ARC represents the curved part of southeastern Hudson Bay and includes the Eastern Hudson Bay, Kuujjuarapik pilot project, and Northeastern Hudson Bay zone of voluntary closure management areas (Figure 2). HS represents the Hudson Strait management area. Note that from 1974-2000, reports from HS also included catches in Ungava Bay. Starting in 2009, reports from HS were given on a spring (HS_{SP}) and fall (HS_{FA}) basis. Then, starting in 2018, harvest reports were provided on a weekly basis, allowing for a finer separation of the fall season into an early (HS_{EF}) and late (HS_{LF}) phases when the estimated proportion of BEL-EHB beluga in the harvest differs. UB_{SP} and UB_{FA} represent the spring and fall harvest in the Ungava Bay management area, respectively. $NEHB_{SP}$ and $NEHB_{FA}$ represent the spring and fall harvest in North East Hudson Bay except for the zone of voluntary closure which is included in the ARC, respectively. The high value of harvest for SAN in 2015 is related to an ice entrapment where all individuals were harvested. Although ice entrapment is a natural event that may result in mortality, here those mortalities were classified as harvest as estimating the proportion that would have died naturally as compared to harvested would be highly uncertain.

YEAR	ARC	SAN	HS	HS_{SP}	HS_{FA}	HS_{EF}	HS_{LF}	UB_{SP}	UB_{FA}	$NEHB_{SP}$	$NEHB_{FA}$	Total
1974	184	0	421	NA	NA	NA	NA	0	0	0	0	605
1975	224	0	586	NA	NA	NA	NA	0	0	0	0	810
1976	216	0	463	NA	NA	NA	NA	0	0	0	0	679
1977	269	14	554	NA	NA	NA	NA	0	0	0	0	837
1978	164	6	243	NA	NA	NA	NA	0	0	0	0	413
1979	271	0	293	NA	NA	NA	NA	0	0	0	0	564
1980	280	0	281	NA	NA	NA	NA	0	0	0	0	561
1981	97	6	236	NA	NA	NA	NA	0	0	0	0	339
1982	114	30	271	NA	NA	NA	NA	0	0	0	0	415
1983	105	7	227	NA	NA	NA	NA	0	0	0	0	339
1984	131	28	189	NA	NA	NA	NA	0	0	0	0	348
1985	103	5	166	NA	NA	NA	NA	0	0	0	0	274
1986	43	25	126	NA	NA	NA	NA	0	0	0	0	194
1987	53	28	125	NA	NA	NA	NA	0	0	0	0	206
1988	52	20	117	NA	NA	NA	NA	0	0	0	0	189
1989	84	19	284	NA	NA	NA	NA	0	0	0	0	387
1990	53	20	109	NA	NA	NA	NA	0	0	0	0	182
1991	106	22	178	NA	NA	NA	NA	0	0	0	0	306
1992	78	20	96	NA	NA	NA	NA	0	0	0	0	194
1993	67	10	189	NA	NA	NA	NA	0	0	0	0	266
1994	82	50	207	NA	NA	NA	NA	0	0	0	0	339
1995	55	30	221	NA	NA	NA	NA	0	0	0	0	306
1996	56	30	211	NA	NA	NA	NA	0	0	0	0	297
1997	51	19	239	NA	NA	NA	NA	0	0	0	0	309
1998	50	54	252	NA	NA	NA	NA	0	0	0	0	356
1999	57	32	238	NA	NA	NA	NA	0	0	0	0	327
2000	62	23	208	NA	NA	NA	NA	0	0	0	0	293
2001	73	27	241	NA	NA	NA	NA	66	0	0	0	407
2002	5	15	161	NA	NA	NA	NA	23	0	0	0	204
2003	8	80	168	NA	NA	NA	NA	26	0	0	0	282
2004	3	94	144	NA	NA	NA	NA	4	0	0	0	245
2005	1	53	172	NA	NA	NA	NA	5	0	0	0	231
2006	0	22	147	NA	NA	NA	NA	2	0	0	0	171
2007	21	24	165	NA	NA	NA	NA	6	0	0	0	216
2008	23	33	92	NA	NA	NA	NA	5	0	0	0	153
2009	21	34	0	68	70	NA	NA	6	0	0	0	199
2010	16	47	0	138	61	NA	NA	8	7	0	0	277
2011	19	32	0	115	86	NA	NA	0	17	0	0	269
2012	13	61	0	208	56	NA	NA	10	2	0	0	350
2013	8	76	0	150	90	NA	NA	8	0	0	0	332
2014	22	26	0	208	37	NA	NA	11	0	1	14	319
2015	36	170	0	106	94	NA	NA	28	3	0	30	467
2016	17	43	0	121	19	NA	NA	24	3	0	3	230
2017	18	30	0	150	85	NA	NA	23	4	0	13	323
2018	14	50	0	146	0	91	0	100	2	2	17	422
2019	35	28	0	144	0	87	23	23	2	2	24	368
2020	39	46	0	189	0	71	7	90	1	0	5	445
2021	28	30	0	51	0	137	23	20	0	0	66	354
2022	19	37	0	161	0	33	90	24	0	25	22	411
2023	17	51	0	225	0	125	56	69	3	15	14	575

Table 4. Proportion of beluga harvested in the different management areas and seasons that are from the BEL-EHB stock used in the IPM. Some seasonal definitions change between regions. Sample size represents the total number of samples collected for genetic analyses (Parent et al. 2023). The 2.5 and 97.5% percentiles of the beta distribution used in the model for prior specification are also shown.

Management area	Season	Sample size	Proportion BEL-EHB	2.5%	97.5%
<i>Nunavik</i>					
East Hudson Bay (ARC)	Summer (Jul. 1 – Aug. 31)	66	0.99 ¹	0.92	1.00
	Spring (Feb. 1 – Aug. 31)	824	0.123	0.10	0.15
Hudson Strait	Fall (Sept. 1 – Jan. 31)	512	0.440	0.40	0.48
	Early Fall (Sept. 1 – Nov. 20)	486	0.461	0.42	0.50
	Late Fall (Nov. 21 – Jan. 31)	49	0.104	0.03	0.21
Ungava Bay	Spring (Feb. 1 – Aug. 31)	143	0.047	0.19	0.09
	Fall (Sept. 1 – Jan. 31)	6	0.168 ²	0.21	0.55
North East Hudson Bay	Spring (Feb. 1 – Aug. 31)	2	0.140 ²	0.35	0.85
	Fall (Sept. 1 – Jan. 31)	45	0.501	0.35	0.65
<i>Nunavut</i>					
Sanikiluaq	Summer (Jul. 1 – Aug. 31)	183	0.99 ¹	0.92	1.00
	Fall (Sept. 1 – Nov. 30)	49	0.610	0.47	0.75
	Winter (Dec. 1 – Mar. 31)	76	0.399	0.29	0.51
	Spring (Apr. 1 – Jun. 30)	229	0.628	0.56	0.69

¹All harvested beluga in those areas in the summer are, by definition, BEL-EHB beluga. A value of 0.99 was used in the model for ease of computation.

²Due to low sample sizes in those harvest categories, we calculated a proportional BEL-EHB contribution based on the fall and spring estimates from Hudson Strait.

Table 5. Description of model parameters and prior distributions.

Parameter	Name	Description	Prior distribution	Value	Lower bound	Upper bound
N_{init}	-	Initial population size	Gamma	α (shape): 1.8; β (rate): 0.0002	1000	30000
ρ	rho	Scaling factor for density dependence on pregnancy rates relative to juvenile survival	Beta	α : 250; β : 250	0	1
η	eta	Base parameter for pregnancy rate	Cauchy	location: 0; scale: 0.5	0	7
γ_0	gamma_0	Baseline log hazard ratio	Half-Cauchy	location: 0; scale: 1	0	10
γ_1	gamma_1	Log hazard ratio for younger ages (early hazards)	Half-Cauchy	location: 0; scale: 1	0	5
γ_2	gamma_2	Log hazard ratio for older ages (late hazards)	Half-Cauchy	location: 0; scale: 1	0	5
γ_3	gamma_3	Log hazard ratio, adult males vs females	Half-Cauchy	location: 0; scale: 0.1	-2	2
γ_h	gamma_h	Mean harvest log hazard	Half-Cauchy	location: 0; scale: 1	0	10
δ	delta	Parameter determining functional form for early hazards	Half-Cauchy	location: 0; scale: 0.1	0	1
ω	omega	Parameter determining functional form for late hazards	Half-Cauchy	location: 0; scale: 0.1	0	1
ψ_1	psi[1]	Age-modifying harvest probability function parameter	Half-Cauchy	location: 0; scale: 1	0	10
ψ_2	psi[2]	Age-modifying harvest probability function parameter	Half-Cauchy	location: 0; scale: 0.1	0	1
ϕ	phi	Density-dependent log hazard ratio	Half-Cauchy	location: 0; scale: 0.01	0	0.5
v_{Pr}	nu_pr	Precision of pregnancy rate proportions	Half-Cauchy	location: 0; scale: 1	0	500
v_{Ag}	nu_ag	Precision of counts by sex and age	Half-Cauchy	location: 0; scale: 5	0	3000
σ_h	sigma_h	Magnitude of variation in hunting hazards	Half-Cauchy	location: 0; scale: 0.1	0	1
σ_e	sigma_e	Magnitude of environmental stochasticity	Half-Cauchy	location: 0; scale: 0.1	0	1
SnL	-	Struck and loss factor	Beta	α : 21.0; β : 56.8	0	1
ξ	xi	Adjustment factor for avoidance by hunters of females with dependent calves	Beta	α : 1; β : 1	0	1

Table 6. Parameter estimate posterior distributions, number of effective samples used, N_{eff} and the \hat{R} statistics, from the IPM for BEL-EHB beluga.

Parameter	Mean	SD	2.5%	50%	97.5%	N_{eff}	\hat{R}
N_{init}	9633	767	8204	9594	11233	327.17	1.04
ρ	0.50	0.02	0.46	0.50	0.54	1856.57	1.00
η	0.94	1.18	0.02	0.49	4.68	1159.34	1.02
γ_0	5.37	0.57	4.09	5.42	6.35	245.30	1.06
γ_1	2.84	0.78	1.36	2.82	4.47	262.66	1.06
γ_2	2.17	0.84	0.38	2.21	3.78	244.95	1.06
γ_3	-0.12	0.09	-0.33	-0.11	0.03	1305.80	1.02
γ_h	7.60	0.14	7.35	7.60	7.88	255.94	1.06
δ	0.10	0.11	0.00	0.06	0.39	890.76	1.02
ω	0.32	0.29	0.01	0.21	0.94	1197.91	1.02
ψ_1	6.43	0.16	6.13	6.43	6.74	846.27	1.03
ψ_2	0.23	0.02	0.20	0.23	0.27	793.59	1.02
ϕ	0.10	0.03	0.05	0.10	0.17	379.62	1.04
v_{Pr}	27.20	20.72	6.71	22.01	79.72	1654.38	1.01
v_{Ag}	1727.91	374.27	1138.68	1677.75	2626.22	1528.84	1.01
σ_h	0.31	0.03	0.26	0.31	0.38	199.53	1.07
σ_e	0.31	0.06	0.25	0.29	0.46	1291.07	1.02
ξ	0.83	0.12	0.55	0.85	0.99	1475.88	1.01

FIGURES

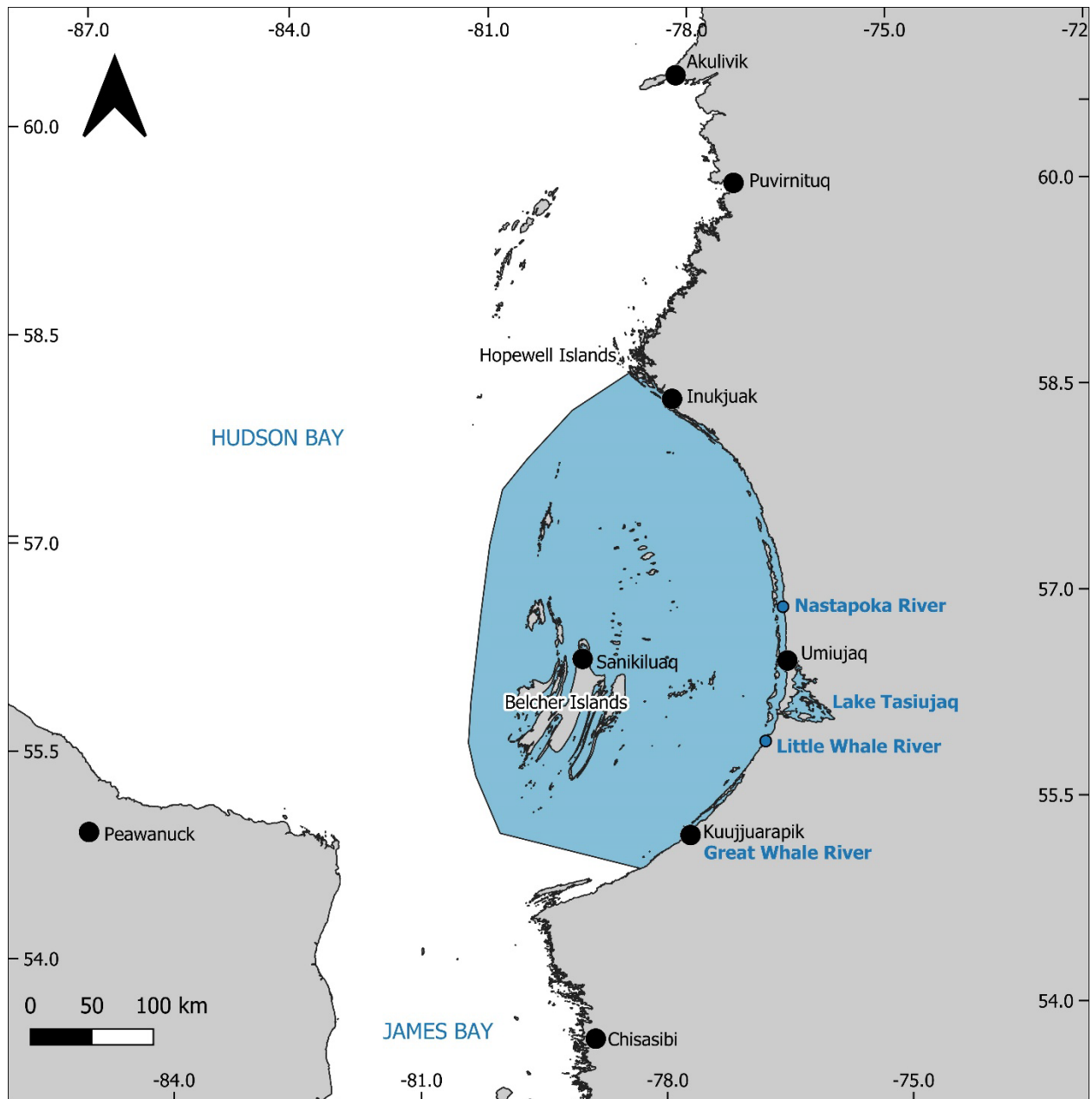


Figure 1. The summer distribution of the BEL-EHB beluga stock (blue polygon) extends from the southeastern Hudson Bay Arc coastline to the east to 60 km west of the Belcher Islands. The Nastapoka River, Great Whale River and Little Whale River estuaries represented historic aggregation areas for the stock, Little Whale River currently appears to be the principal site for beluga aggregations in the eastern Hudson Bay Arc.

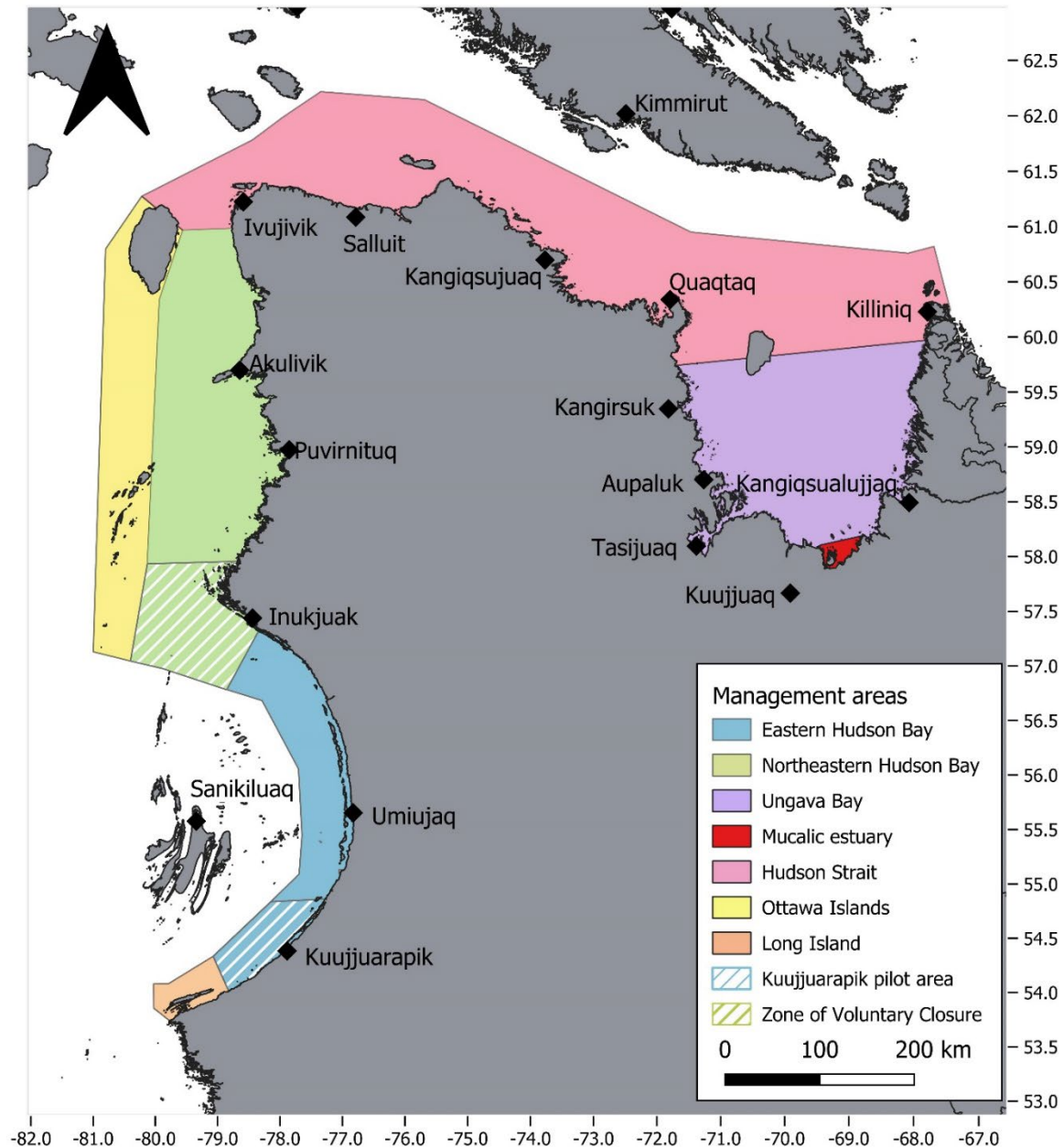


Figure 2. Map of communities (black) and management areas in Nunavik, Québec, Canada. In the present BEL-EHB beluga IPM, we assigned reported harvest data to four management areas in Nunavik: 1) the “Arc”, which comprises Eastern Hudson Bay including the Kuujjuarapik pilot area and the Zone of Voluntary Closure, 2) Northeastern Hudson Bay (except the Zone of voluntary closure), 3) Hudson Strait and Ungava Bay. No harvest were reported in Ottawa Islands. The IPM also accounts for harvest in Sanikiluaq, which is located on the Belcher Islands and is part of Nunavut. The Long Island, Belcher Islands and Arc areas are summering grounds for the James Bay, BEL and EHB beluga genetic populations, respectively. Therefore, all beluga harvested in Sanikiluaq and the Arc during summer (i.e., July and August) are considered taken from the BEL-EHB beluga stock. Similarly, all beluga harvested in Long Island during summer are deemed James Bay beluga. In other seasons and management areas, the genetic composition of the harvest was used to calculate the BEL-EHB mortality associated with harvest.

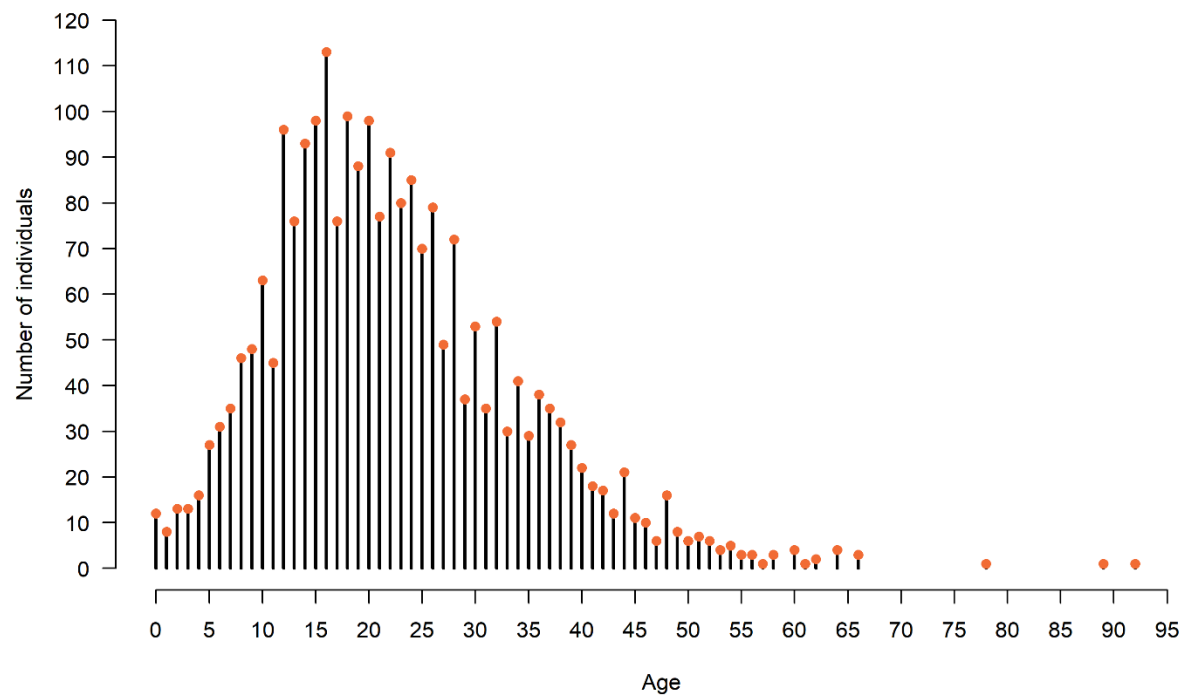


Figure 3. Age distribution of beluga sampled during harvest in Nunavik, 1980-2022. Note that for ease of visualization, the data has been aggregated across years here, but is used on an annual basis in the model.

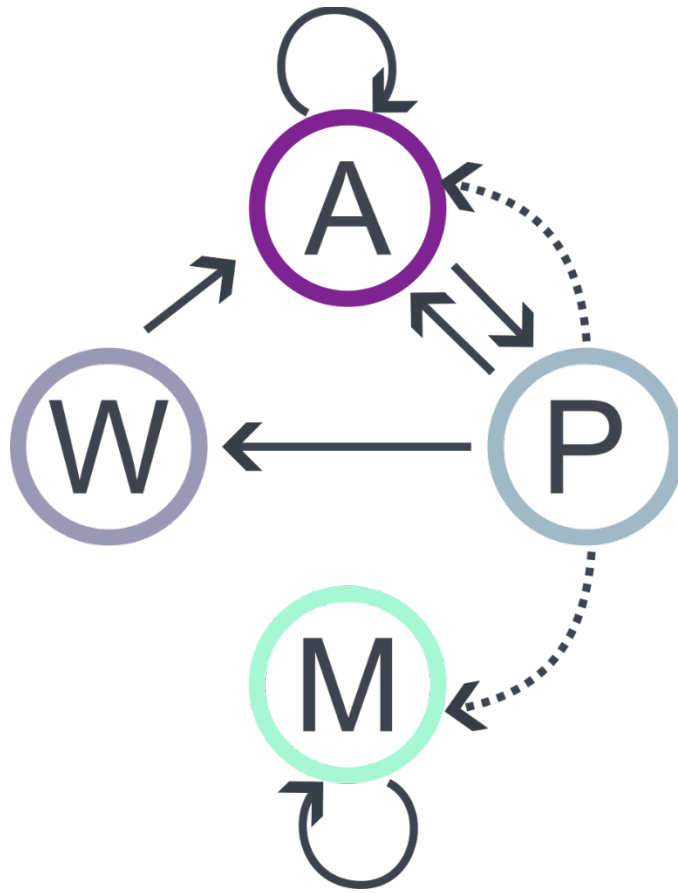


Figure 4. Life cycle graph of the beluga, showing annual state transitions (solid lines) and production of new individuals (dashed lines) Definitions: M: males, A: non-reproducing females, P: pregnant females, W: females with a calf.

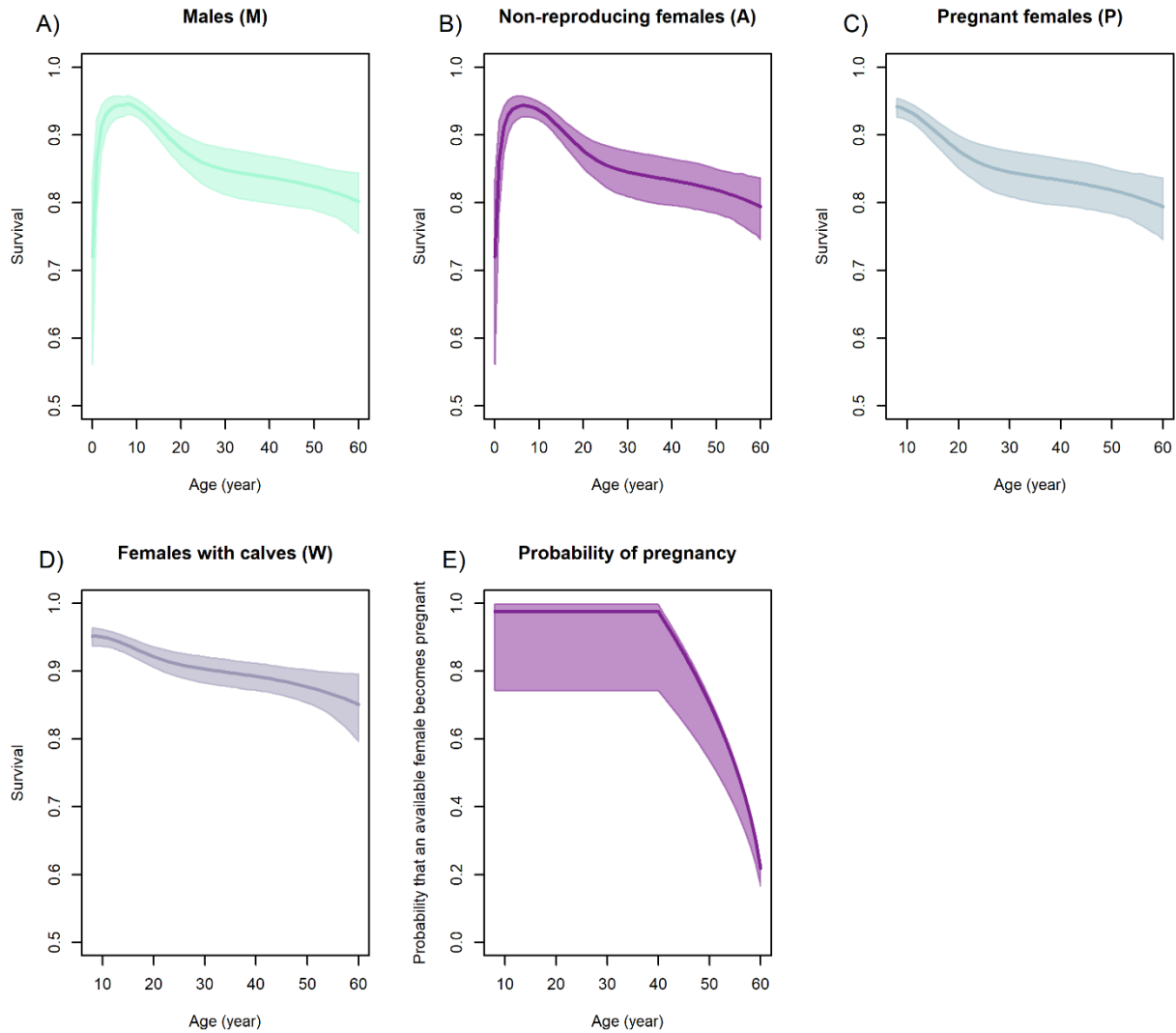


Figure 5. Age-specific demographic rates (survival and probability of pregnancy) estimated by the multistate Integrated Population Model for the BEL-EHB beluga stock in Nunavik, Canada. On the graph is an example for year 2023.

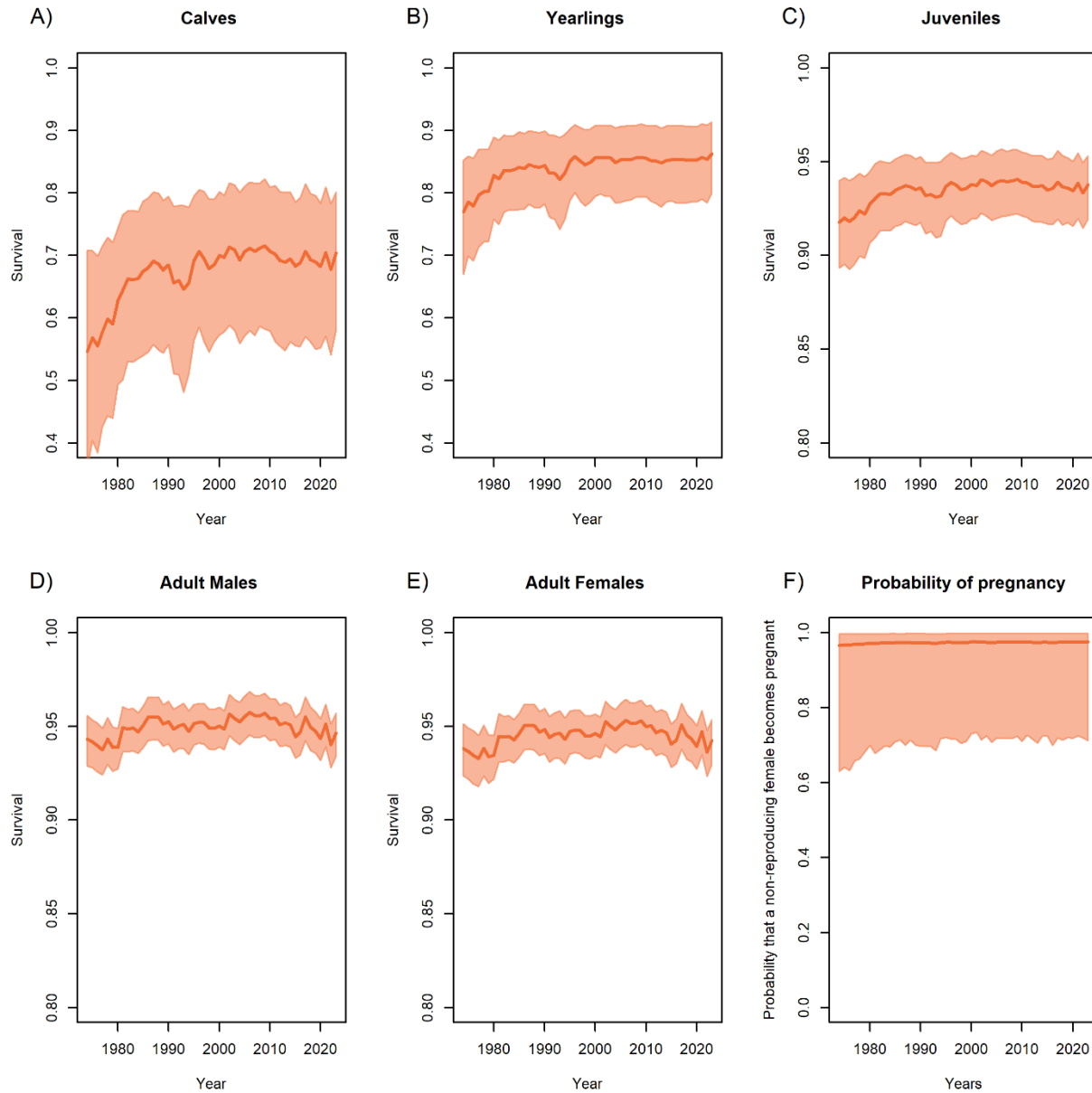


Figure 6. Temporal variation in demographic rates estimated by the multistate Integrated Population Model for the BEL-EHB beluga stock in Nunavik, Canada. The dark orange line and the light orange polygon represent the mean and 95% Credible Intervals of the posterior distribution, respectively. Survival trends were estimated for calves (age 0), yearlings (age 1 year old), juveniles (age 5 years old is shown here), adult males and females (age 8 years-old is shown here). Probability of pregnancy represents the probability that a female becomes pregnant at year $t + 1$, conditional on her being available to mate at year t .

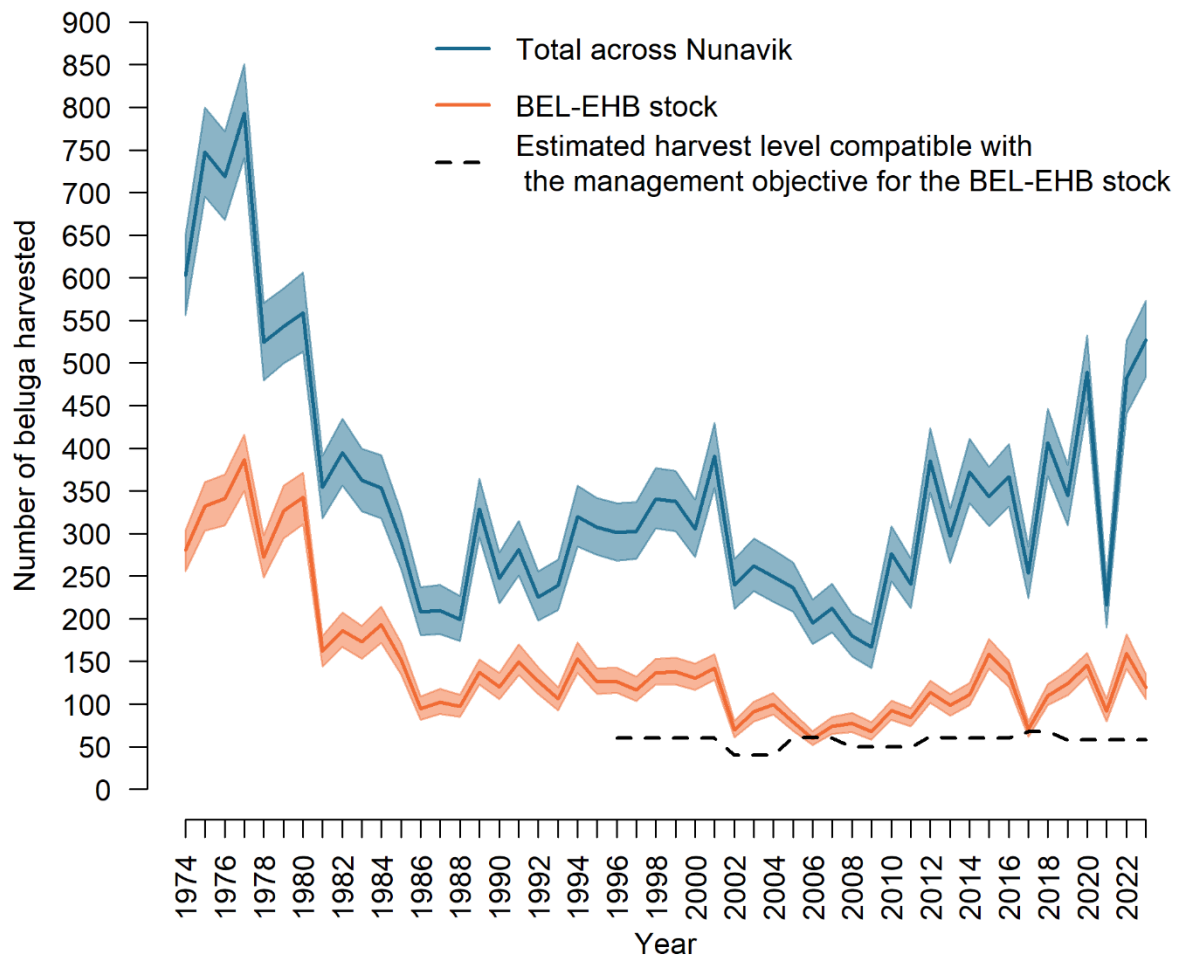


Figure 7. Temporal variation in number of beluga landings across Nunavik and specifically from the BEL-EHB stock, as estimated by the multistate Integrated Population Model. Solid lines represent the mean and the shaded areas are the 95% Credible Interval from the posterior distributions. The estimated harvest levels compatible with the management objectives for the BEL-EHB stock, which have varied over time, are also provided (dashed line) for reference.

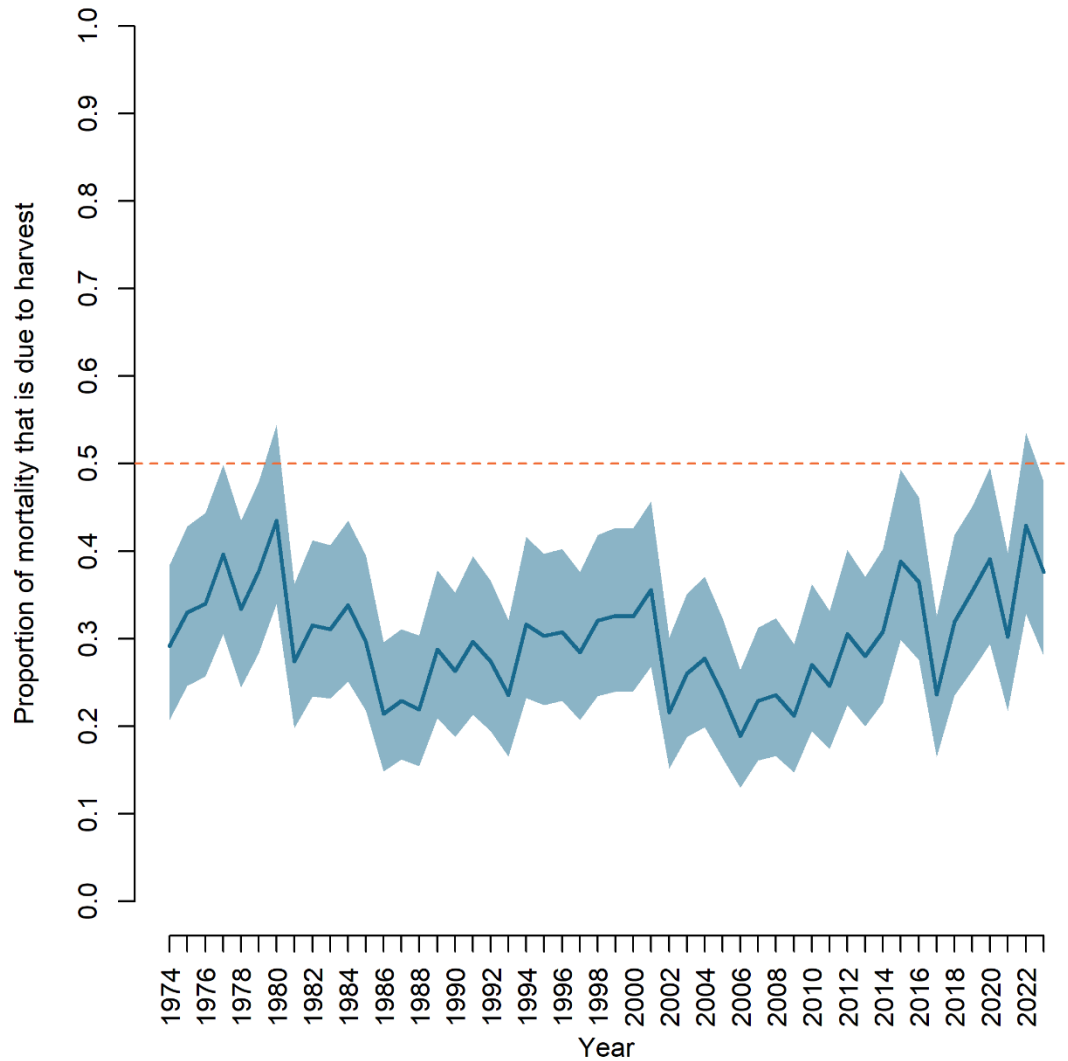


Figure 8. Temporal variation in the relative proportion of total mortality that is due to harvest, including animals that were landed and reported as well as those that were struck and lost (i.e., unrecovered or not reported), estimated by the multistate Integrated Population Model for BEL-EHB beluga. The horizontal dashed orange line shows the 50% line. Solid blue line represents the mean and the shaded area is the 95% Credible Interval from the posterior distribution.

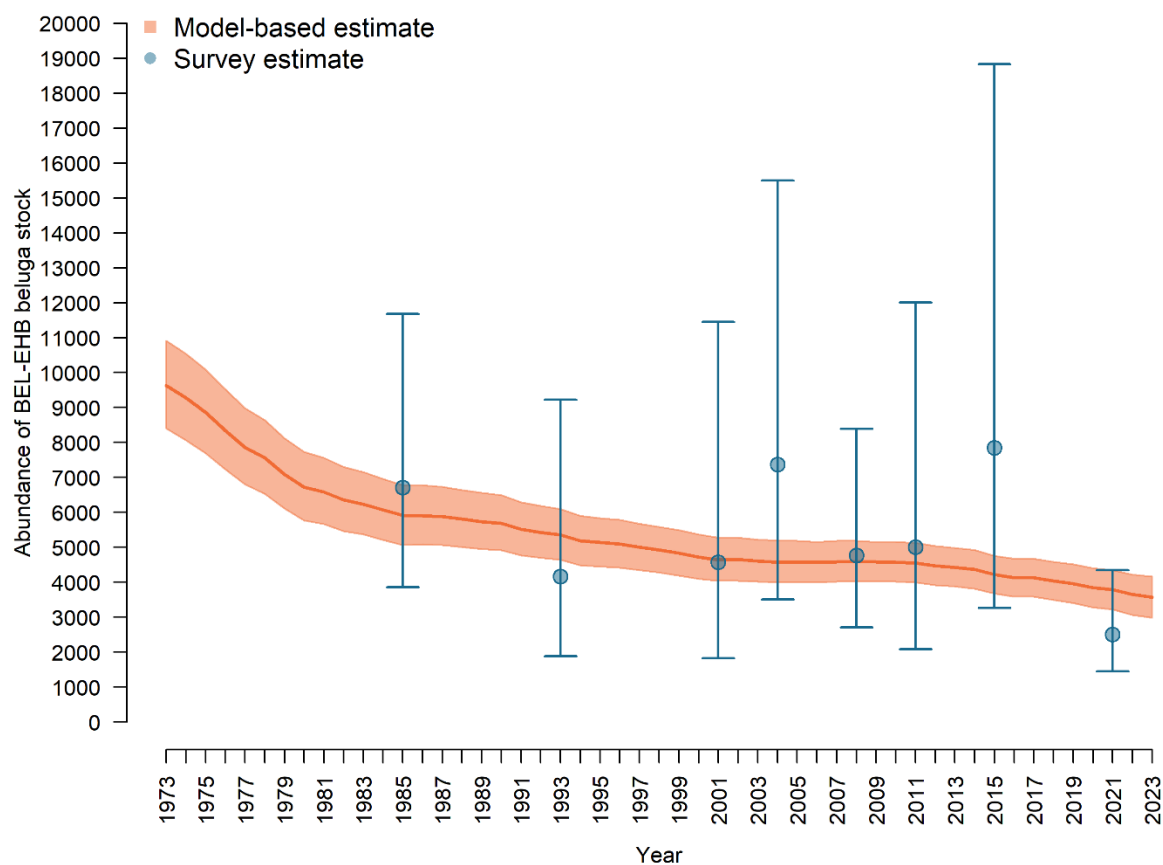


Figure 9. Demographic trend for the BEL-EHB beluga stock in Nunavik, Quebec, Canada. Abundance (mean: dark orange line, 95% Credible Interval: light orange polygon) is estimated from a multistate (age times state) Integrated Population Model informed by periodic aerial survey estimates (mean: blue dots, 95% Confidence Intervals: blue arrows), annual pregnancy rates and age/sex structure in the harvest.

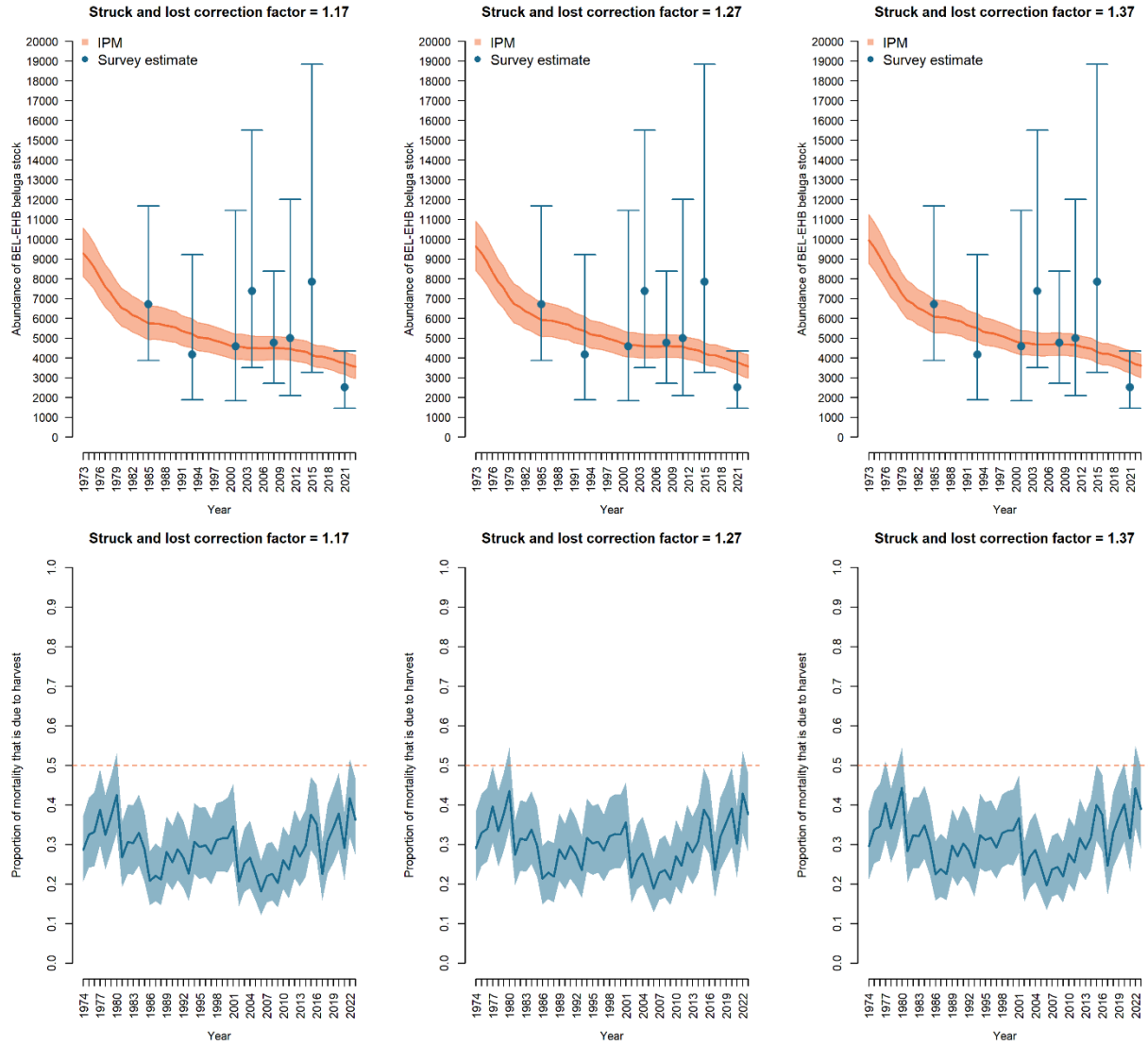


Figure 10. Impact of changing struck and loss value on abundance (upper panels) and the contribution of harvest to overall mortality for BEL-EHB beluga stock.

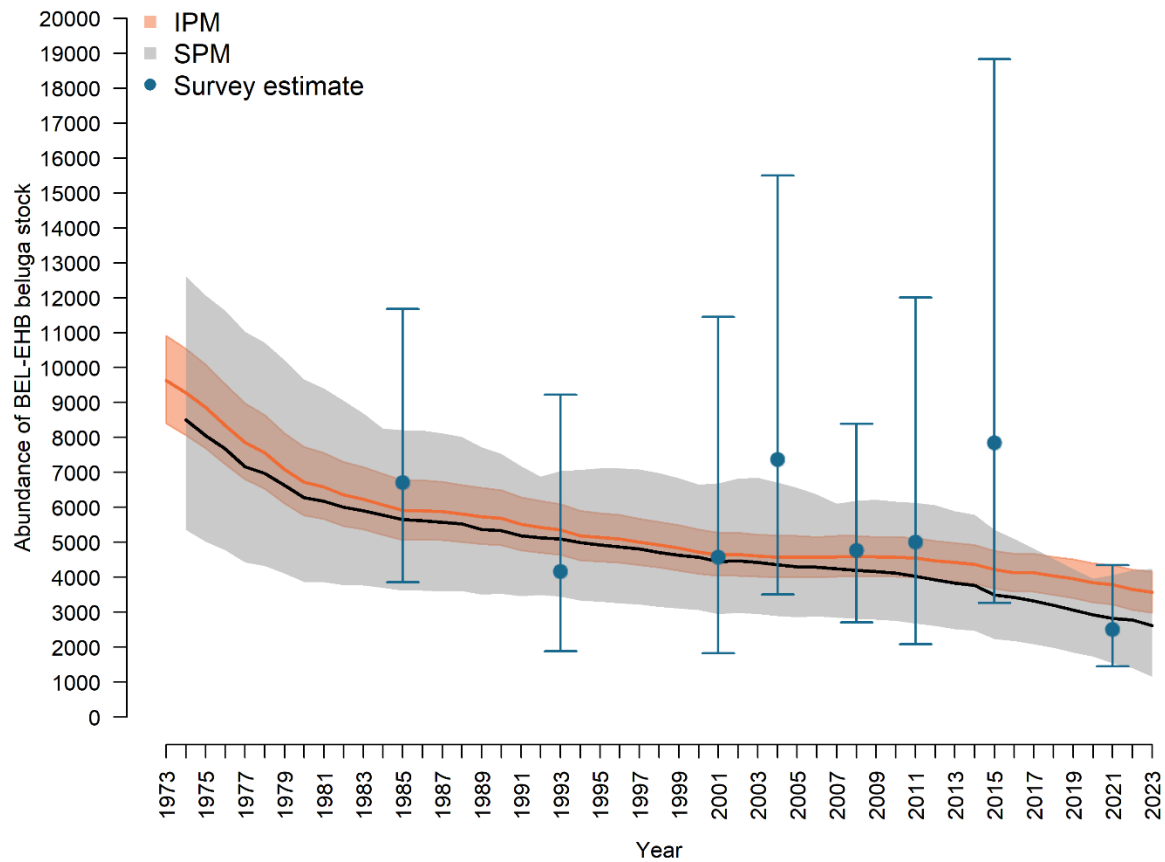


Figure 11. Comparison of BEL-EHB beluga stock abundance between the IPM and SPM (Hammill et al. 2023b; Sauvé et al. 2024) model formulations. Abundance (solid lines) and 95% Credible Interval (shaded areas) are shown for each model (IPM: orange, SPM: black and grey). Periodic aerial survey estimates are shown in blue along with 95% Confidence Intervals.

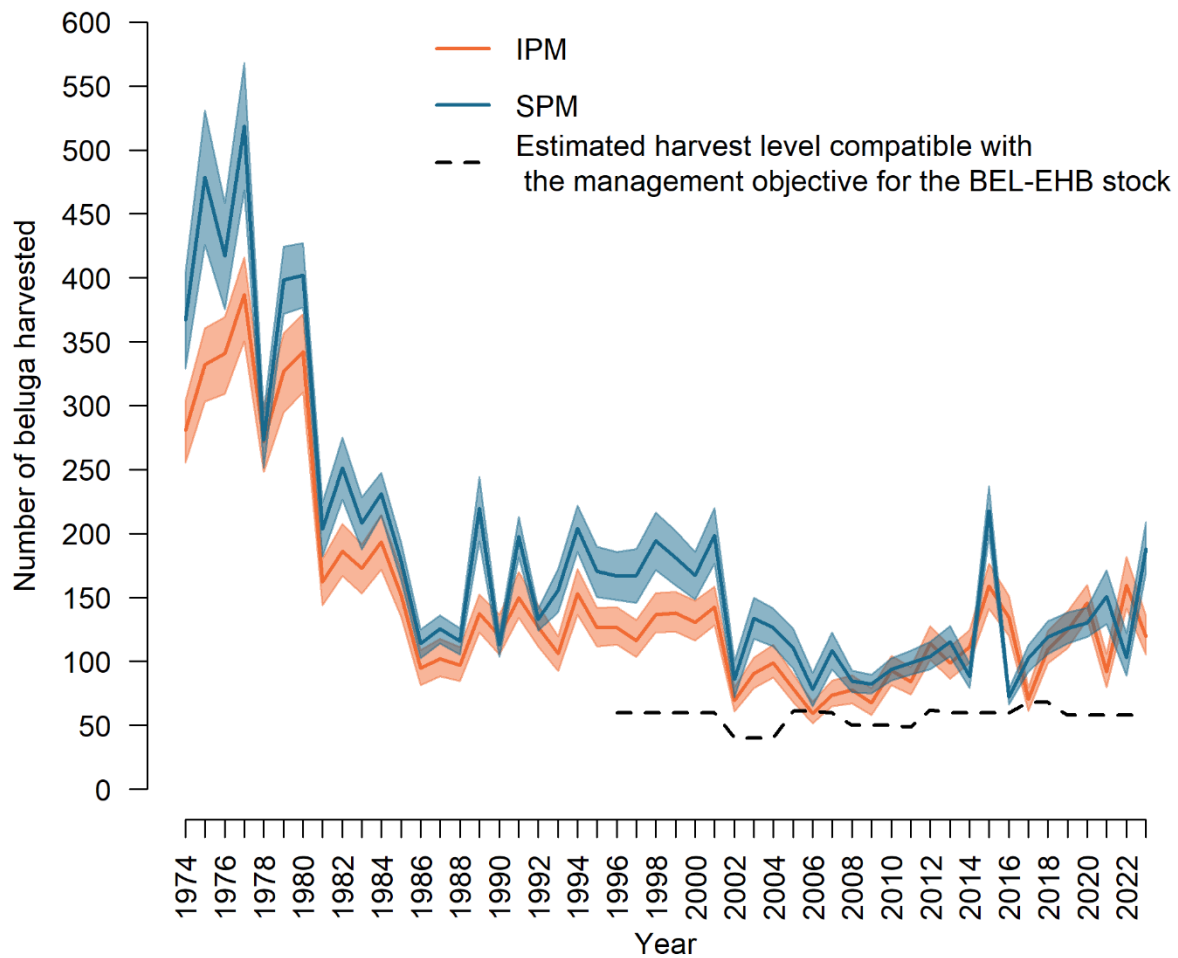


Figure 12. Comparison of model-based estimates of number of BEL-EHB beluga landings across years between the IPM and SPM. Solid lines represent the mean and the shaded areas are the 95% Credible Interval from the posterior distributions. The estimated harvest levels compatible with the management objective for the BEL-EHB stock, which have varied over time, are also provided (dashed line) for reference.

APPENDIX

MULTISTATE MODEL CONSTRUCTION

The vector of population size $\tilde{\mathbf{n}}$ has age classes i arranged within states j , with the entry $\tilde{\mathbf{n}}_{ij}$ corresponding to the number of individuals within age class i and state j :

$$\tilde{\mathbf{n}} = \begin{pmatrix} n_{11} \\ \vdots \\ n_{w1} \\ - \\ n_{21} \\ \vdots \\ n_{w2} \\ - \\ \vdots \\ - \\ n_{1b} \\ \vdots \\ n_{wb} \end{pmatrix} \quad (\text{A1})$$

The matrix $\tilde{\mathbf{A}}$ can be decomposed into its constituents as follows:

$$\tilde{\mathbf{A}} = \tilde{\mathbf{U}} + \tilde{\mathbf{F}} \quad (\text{A2})$$

$\tilde{\mathbf{A}}$, $\tilde{\mathbf{U}}$, and $\tilde{\mathbf{F}}$ are all of dimension $wb \times wb$. The matrix $\tilde{\mathbf{U}}$ contains transition probabilities for living individuals, and $\tilde{\mathbf{F}}$ contains the production of new individuals by mature individuals.

Transitions within $\tilde{\mathbf{U}}$ and $\tilde{\mathbf{F}}$ are further decomposed into distinct processes, each occurring in the distinct model dimensions (here two dimensions: age, and state). For instance, $\tilde{\mathbf{U}}$ combines two distinct processes:

1. transitions between age classes included in the block-diagonal matrix \mathbf{U} , and
2. transition between states included in the block-diagonal matrix \mathbf{B} .

The matrix $\tilde{\mathbf{F}}$ combines

1. production of offspring included in the block-diagonal matrix \mathbf{R} ,
2. classification of offspring into the first breeding state included in the block-diagonal matrix \mathbf{F} .

TRANSITIONS OF LIVE INDIVIDUALS

The hyperstate matrix $\tilde{\mathbf{U}}$ is obtained by sequentially multiplying the two sub-processes:

$$\tilde{\mathbf{U}} = \mathbf{K}^T \mathbb{B} \mathbf{K} \mathbf{U} \quad (\text{A3})$$

Each sub-process is captured by its corresponding block-diagonal matrix \mathbf{U} and \mathbb{B} , respectively, which are also of dimension $wb \times wb$. Reading from right to left, individuals will move between dimensions at each time step following this specific sequence of transitions

1. age classes through \mathbf{U} and
2. breeding state through \mathbb{B} .

The vec-permutation matrix \mathbf{K} rearranges the vector $\tilde{\mathbf{n}}$ for the matrix multiplication in the next dimension. Note that \mathbf{K}^T is the transpose of the matrix \mathbf{K} .

The matrix \mathbb{U} has matrices \mathbf{U}_j arranged on its diagonal,

$$\mathbb{U} = \begin{pmatrix} \mathbf{U}_1 & \mathbf{0} & \mathbf{0} & \mathbf{0} \\ \mathbf{0} & \mathbf{U}_2 & \mathbf{0} & \mathbf{0} \\ \mathbf{0} & \mathbf{0} & \mathbf{U}_3 & \mathbf{0} \\ \mathbf{0} & \mathbf{0} & \mathbf{0} & \mathbf{U}_4 \end{pmatrix} \quad (\text{A429})$$

and is obtained using the following equation:

$$\mathbb{U} = \sum_{j=1}^{s/s_d} \mathbf{E}_{jj} \otimes \mathbf{U}_j \quad (\text{A5})$$

where s is product of dimensions, i.e., $s = w \times b$ and s_d is the size of the dimension of interest, i.e., in the case of the \mathbf{U}_j matrices, $s_d = w$. Note that block matrices \mathbb{B} , \mathbb{R} , and \mathbb{F} (see section “Reproduction processes” below) are constructed in the same way. The matrices \mathbf{U}_j are of dimension $w \times w$. For a given breeding state j the matrix \mathbf{U}_j moves individuals between age classes i according to their age-, and state-specific survival rates S_{ij} (see equation 2 in the main text).

The matrix \mathbb{B} has a similar structure to \mathbb{U} , but with matrices \mathbf{B}_i on the diagonal. The \mathbf{B}_i matrices move individuals between the four breeding states (M, A, P, W) for each age class (i) according to probabilities of become pregnant and losing the calf (see equation 3 in the main text).

REPRODUCTION PROCESSES

The hyperstate matrix $\tilde{\mathbf{F}}$ is obtained by multiplying the two sub processes:

$$\tilde{\mathbf{F}} = \mathbf{K}^T \mathbf{F} \mathbf{K} \mathbb{R} \quad (\text{A6})$$

Reading from right to left, individuals will produce offspring at each time step following this specific sequence of transitions

1. production of individuals of age class 1 through \mathbb{R} and
2. classification of age class 1 individuals within the male and non-reproducing female state through \mathbb{F} .

The vec-permutation matrices \mathbf{K} here again rearrange the dimensions of each of these matrices to respect matrix organization at each step of the multiplication.

The matrix \mathbb{R} has matrices \mathbf{R}_j arranged on the diagonal. For each breeding state j , the \mathbf{R}_j matrices capture the production of offspring (all in the first age class or first row) from individuals within each of the adult age classes (see equation 4 in the main text).

As a result of this process, all newly produced offspring are classified within the age class 1, but they remain classified within the breeding state category of their mother ($j = 3$).

Reclassification of the newly produced offspring within the male (M) or non-reproducing female (F) states is achieved using the matrix \mathbb{F} . The matrix \mathbb{F} contains the \mathbf{F}_i matrices on its diagonal. Matrices \mathbf{F}_i are of dimension $b \times b$ and put back within the male (M) or non-reproducing female (F) state the offspring coming from pregnant females (see equation 5 in the main text).

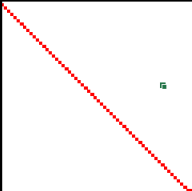
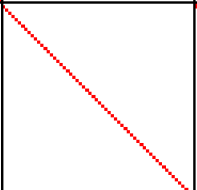
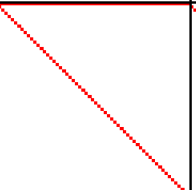
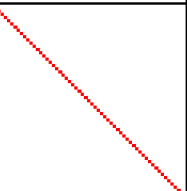
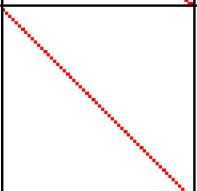
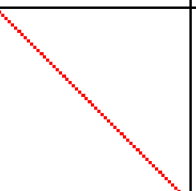
	Males	Available females	Pregnant females	Females with calves
Males				
Available females				
Pregnant females				
Females with calves				

Figure A1. Multistate projection matrix visual representation. Non-zero (or parameterized) entries are shown in red.

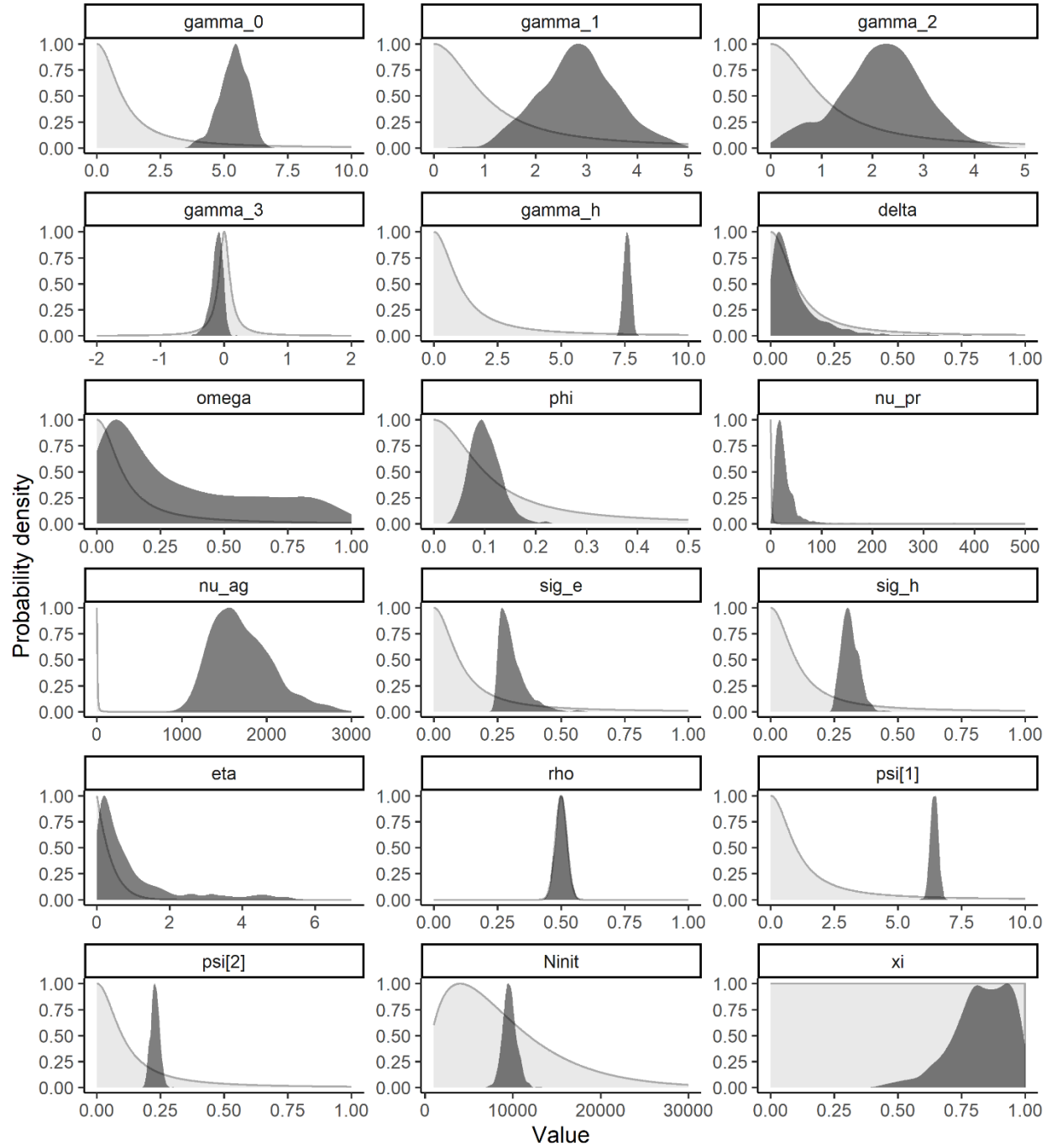


Figure A2. Prior (light grey) and posterior (dark grey) distribution of IPM parameters.

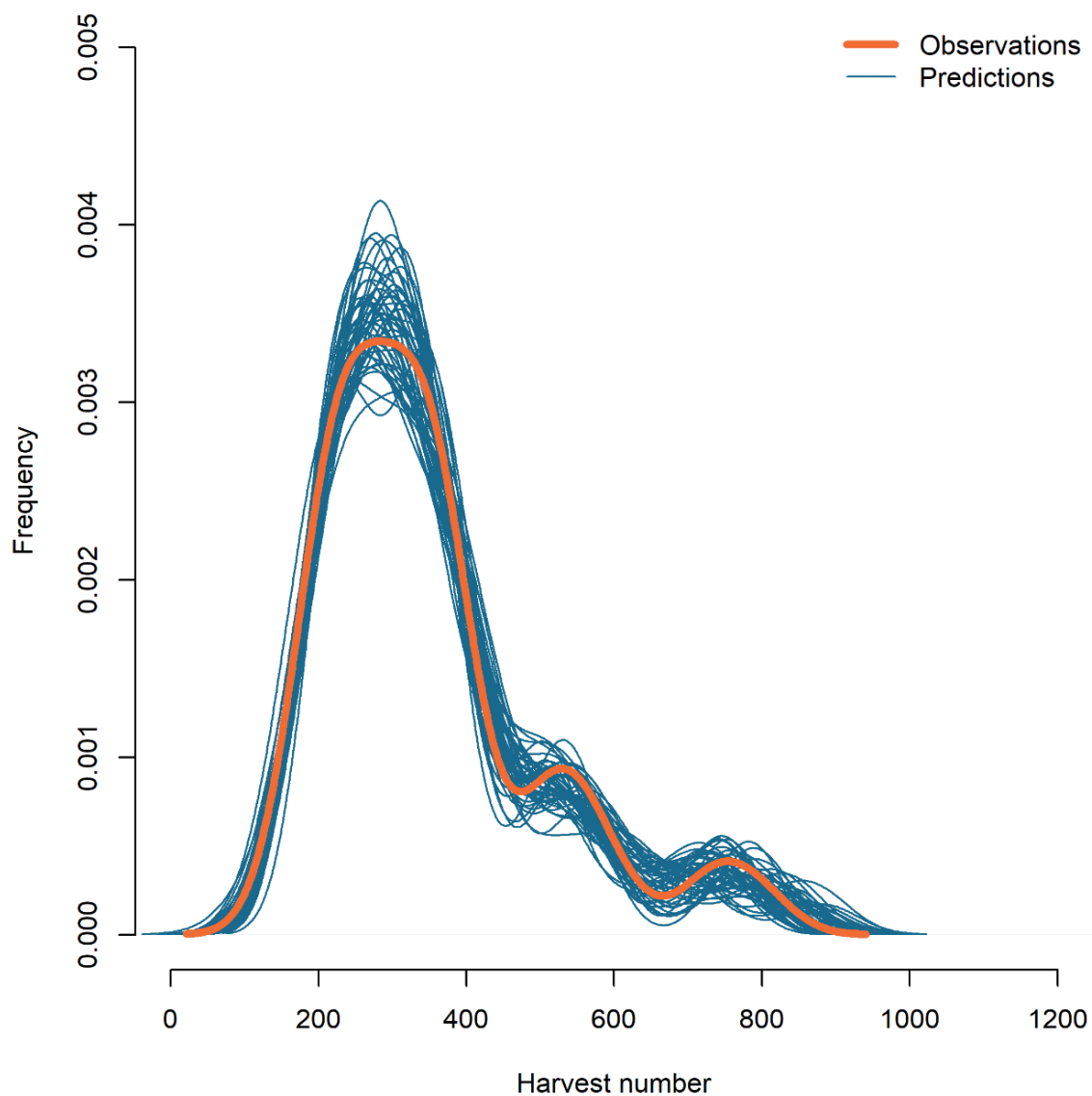


Figure A3. Comparison between the observed number of beluga harvested annually and the out-of-sample predictions. For ease of visualization, only 50 randomly chosen predictions are presented.

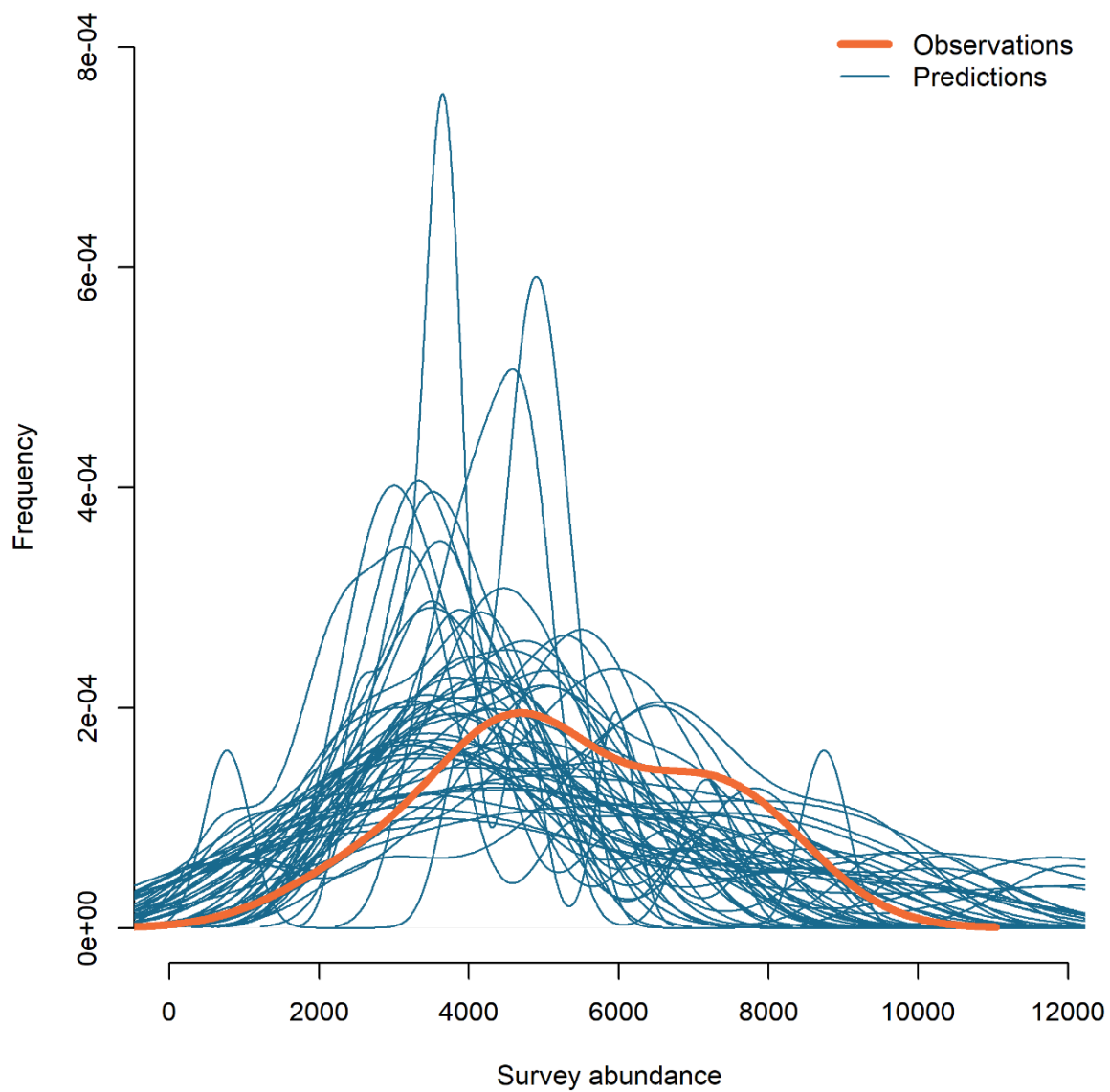


Figure A4. Comparison between the observed abundance of beluga(aerial surveys) annually and the out-of-sample predictions. For ease of visualization, only 50 randomly chosen predictions are presented.

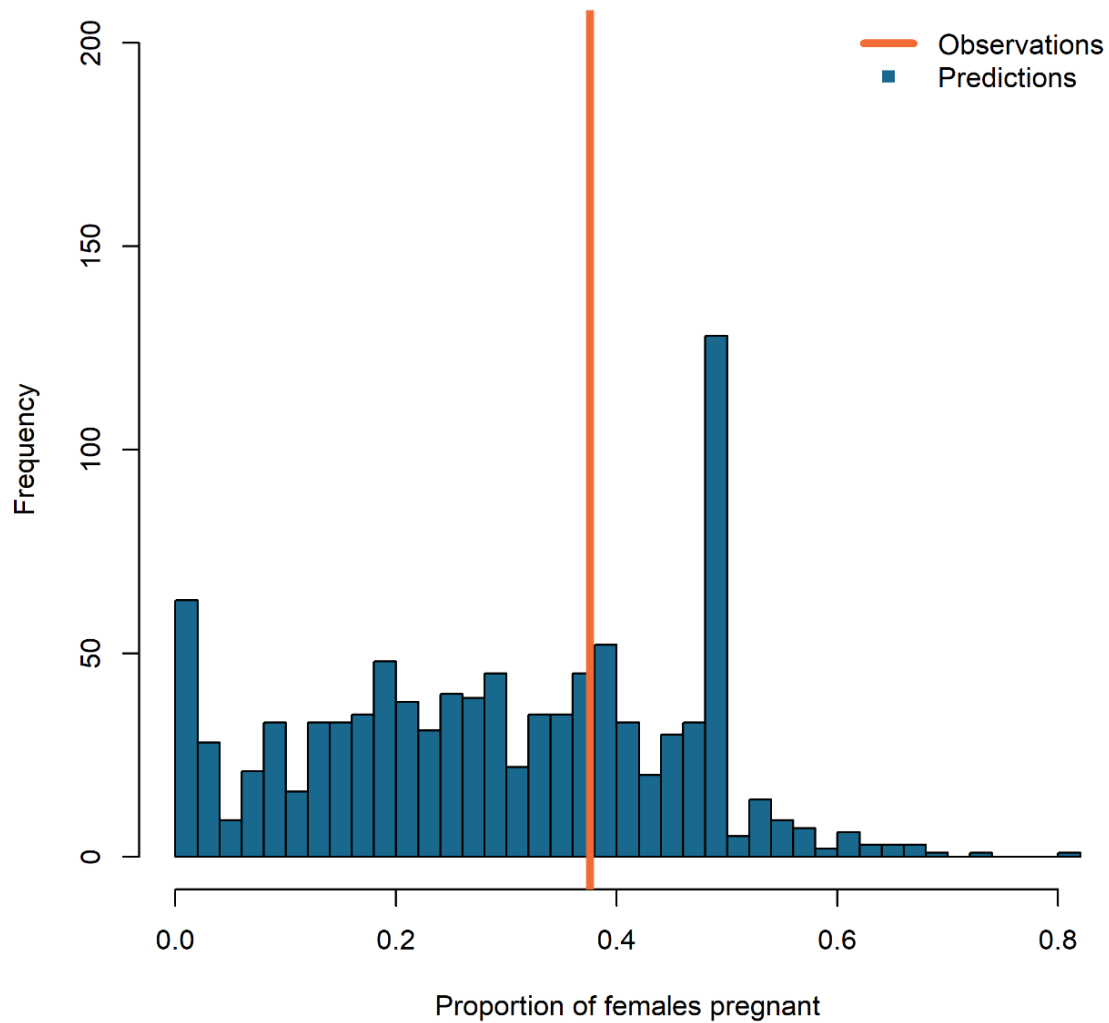


Figure A5. Comparison between the observed proportion of pregnant females and the out-of-sample predictions. Medians across years are shown.

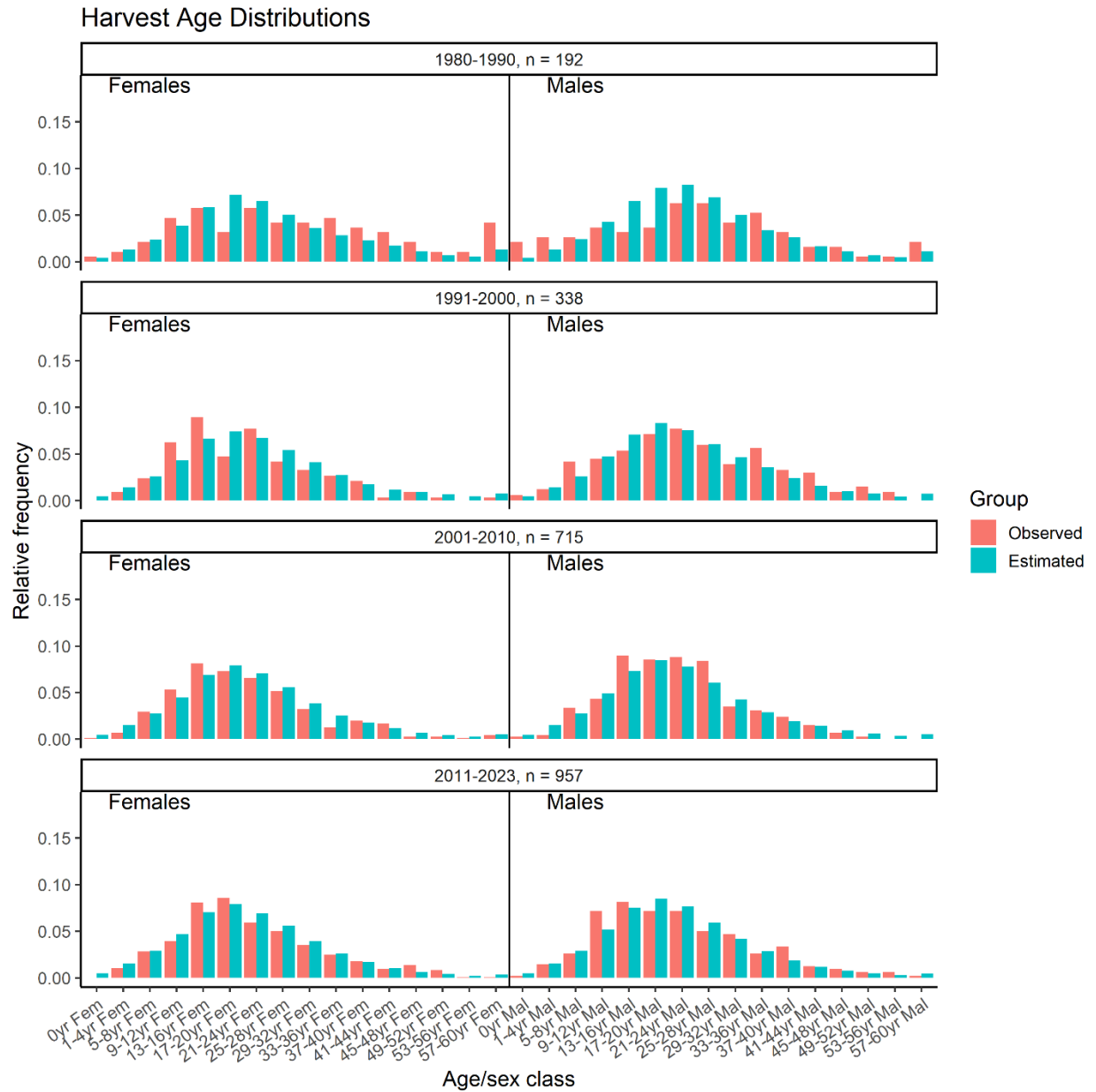


Figure A6. Observed (orange) and estimated by the IPM (blue) age and sex distributions for four time periods (1980-1990, 1991-2000, 2001-2010 and 2011-2023).

Posterior predictive check, sum of squared Pearson residuals
Bayesian-P = 0.43

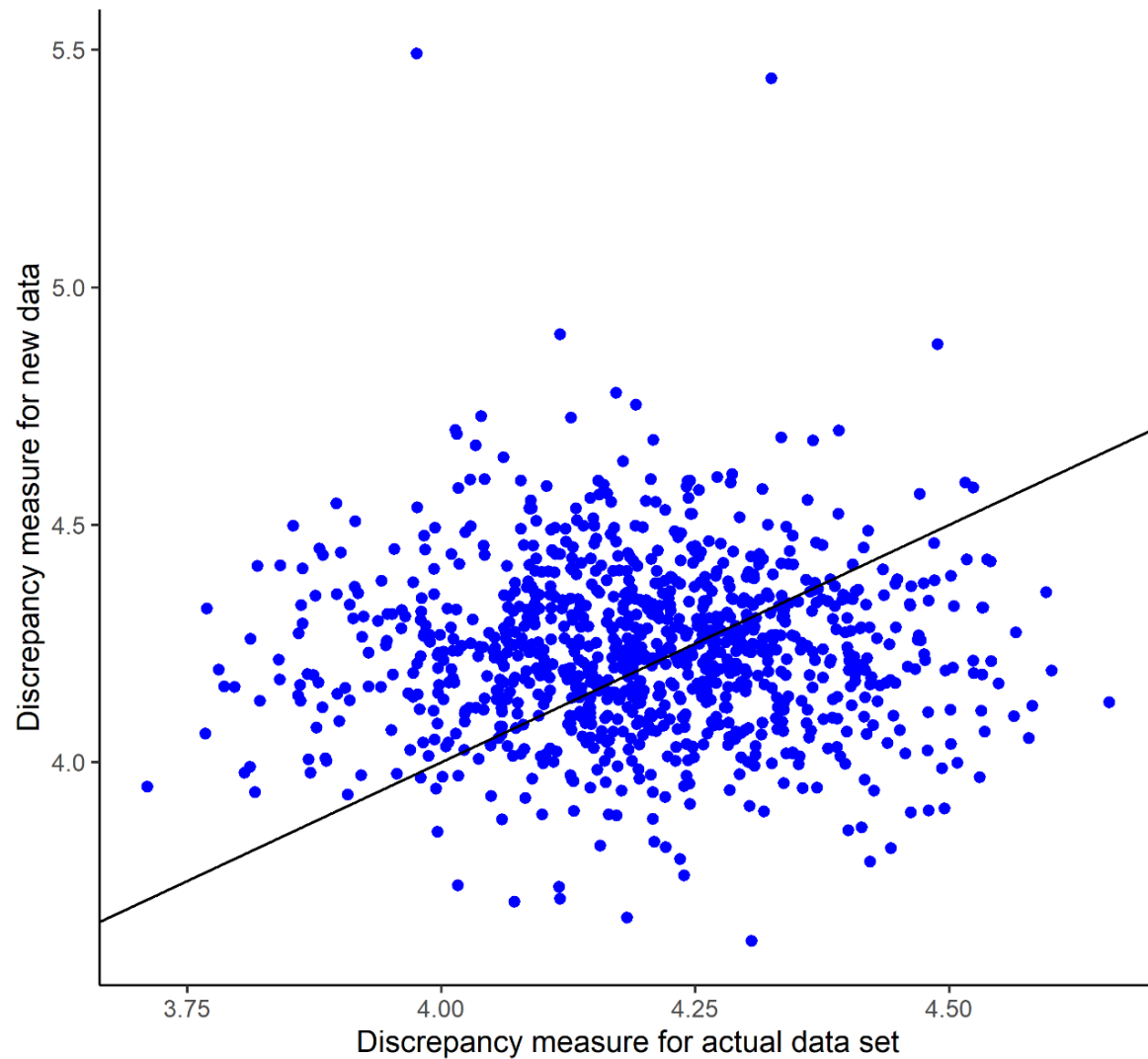


Figure A7. Correlation between sum of squared residuals between observations and model-based predictions for the IPM.

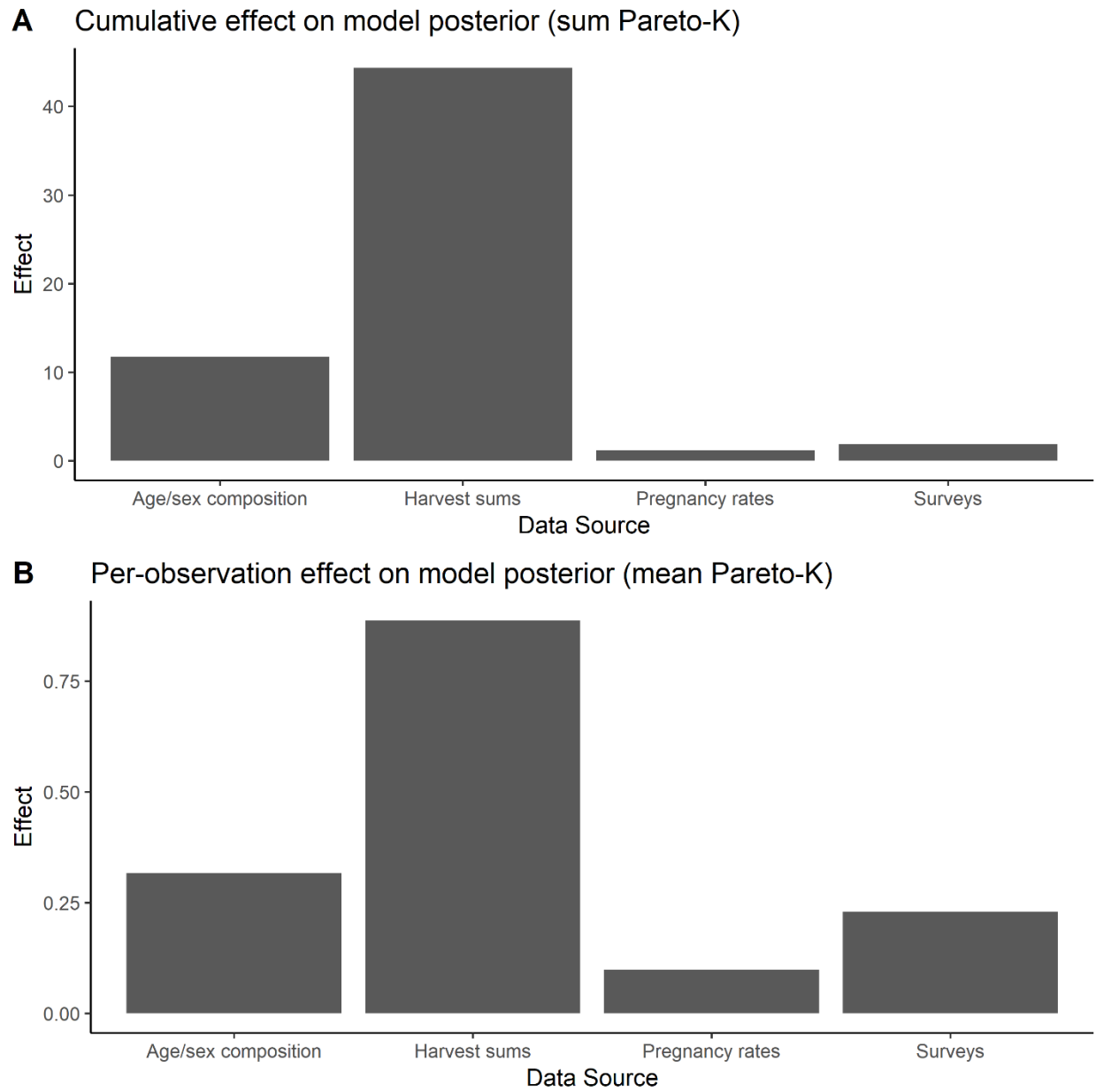


Figure A8. Relative cumulative (A) and per-observation (B) contribution of the four main data sources to IPM estimates.